

Highlights

RE-LLM: Integrating Large Language Models into Renewable Energy Systems

Ali Forootani*, Mohammad Sadr, Danial Esmaeili Aliabadi, Daniela Thrän

- RE-LLM integrates optimization, ML surrogates, and LLMs for energy planning.
- Machine learning surrogates accelerate scenario analysis while retaining fidelity.
- LLM-generated narratives improve comprehension beyond charts and tables.
- Framework enhances transparency and accessibility for policy and stakeholders.
- Demonstrated on Germany’s land-based GHG mitigation strategies (2020–2050).

RE-LLM: Integrating Large Language Models into Renewable Energy Systems

Ali Forootani^{*a}, Mohammad Sadr^a, Danial Esmaeili Aliabadi^a, Daniela Thrän^{a,b,c}

^a*Helmholtz Centre for Environmental Research - UFZ, Permoserstraße 15, 04318 Leipzig, Germany*

^b*DBFZ Deutsches Biomasseforschungszentrum gGmbH, Torgauer Strasse 116, 04347 Leipzig, Germany*

^c*University Leipzig, Institute for Infrastructure and Resources Management, Grimmaische Str. 12, 04109 Leipzig, Germany*

Abstract

Energy system models are increasingly employed to guide long-term planning in multi-sectoral environments where decisions span electricity, heat, transport, land use, and industry. While these models provide rigorous quantitative insights, their outputs are often highly technical, making them difficult to interpret for non-expert stakeholders such as policymakers, planners, and the public. This communication gap limits the accessibility and practical impact of scenario-based modeling, particularly as energy transitions grow more complex with rising shares of renewables, sectoral integration, and deep uncertainties.

To address this challenge, we propose the Renewable Energy Large Language Model (RE-LLM), a hybrid framework that integrates Large Language Models (LLMs) directly into the energy system modeling workflow. RE-LLM combines three core elements: (i) optimization-based scenario exploration, (ii) machine learning surrogates that accelerate computationally intensive simulations, and (iii) LLM-powered natural language generation that translates complex results into clear, stakeholder-oriented explanations. This integrated design not only reduces computational burden but also enhances inter-

^{*}Ali Forootani

Email addresses: ali.forootani@ufz.de/aliforootani@ieee.org (Ali Forootani^{*}), mohammad.sadr@ufz.de (Mohammad Sadr), danial.esmaeili@ufz.de (Danial Esmaeili Aliabadi), daniela.thraen@ufz.de (Daniela Thrän)

pretability, enabling real-time reasoning about trade-offs, sensitivities, and policy implications.

The framework is adaptable across different optimization platforms and energy system models, ensuring broad applicability beyond the case study presented. By merging speed, rigor, and interpretability, RE-LLM advances a new paradigm of human-centric energy modeling. It enables interactive, multilingual, and accessible engagement with future energy pathways, ultimately bridging the final gap between data-driven analysis and actionable decision-making for sustainable transitions.

Keywords: Renewable energy, Scenario modeling, Machine learning, Large language models, Interpretability, Optimization, Stakeholder analysis

1. Introduction

Energy system models have become indispensable decision-support tools for strategic planning and policy design in the face of climate change, rising energy demand, and the global pursuit of carbon neutrality. By casting long-term investment and technology-deployment questions as large-scale optimization problems—most commonly linear programming (LP), mixed-integer linear programming (MILP), or dynamic programming (DP) Forootani et al. [1]—these models identify cost-optimal or emissions-minimizing pathways across interconnected energy sectors such as electricity, heat, transport, and other non-energy sectors Howells et al. [2], Bhattacharyya [3], Laveneziana et al. [4], Dagoumas and Koltsaklis [5], Connolly et al. [6], Ringkjøb et al. [7].

The smooth transition to low-carbon, renewables-dominated energy systems therefore relies on robust decision-making frameworks, such as TIMES Loulou et al. [8], MESSAGE Huppmann et al. [9], and OSeMOSYS Howells et al. [2]. These scenario-based models integrate detailed techno-economic inputs with policy and demand uncertainties, solving cost-minimization or utility-maximization problems to reveal cost-effective technology portfolios, investment schedules, and policy interventions at various spatiotemporal resolutions and regions. Yet, as energy systems grow in complexity—due to increasing penetration of variable renewables, sector coupling, and decentralized generation—there is a rising demand for *modular, multi-sectoral, and high-resolution models*. Tools such as GENeSYS-MOD Löffler et al. [10], Barani et al. [11], PyPSA Brown et al. [12], BENOPTex Millinger et al. [13] and Calliope

Pfenninger and Pickering [14] have emerged to support these requirements by offering open-source, flexible, and highly customizable modeling environments. These frameworks support scenario construction, multi-region trade analysis, and sensitivity studies, often with transparent data structures and scripting interfaces in Python or GAMS.

Despite their analytical power, these complex (optimization or equilibrium) models tend to produce results in the form of large tabular datasets and configuration files, which can be consumed by machines, but are not easily interpretable by non-expert stakeholders Vaidyanathan [15]. This has motivated the integration of scenario analysis tools that go beyond numerical outputs, facilitating the exploration of counterfactuals, trade-offs, and pathway comparisons. Scenario explorers such as IIASA’s Scenario Explorer Cointe [16], Huppmann et al. [17], IAMC’s databases Huppmann et al. [17], and En-ROADS Rooney-Varga et al. [18] enable interactive exploration of pre-computed trajectories under different assumptions.

1.1. Comparison of Energy System Optimization Frameworks

The literature on renewable energy system optimization can be broadly categorized into the following themes:

- (i) Integrated Assessment Models (IAMs): Studies using tools such as MESSAGE-GLOBIOM van Ruijven and Min [19], Rogelj et al. [20] and REMIND-MagPIE combine energy Klein et al. [21], land, and climate modules to assess global climate targets. These models have been instrumental in producing scenarios for the IPCC and informing global mitigation pathways.
- (ii) National Energy Planning: Optimization frameworks tailored for country-level planning (e.g., UK TIMES Loulou et al. [22], McJeon et al. [23], ReEDS Short et al. [24], GENesYS-MOD Germany Löffler et al. [25]) explore cost-optimal decarbonization strategies while accounting for local resource potentials, technology roadmaps, and policy constraints.
- (iii) Multi-Sector Coupling: Recent work emphasizes sectoral integration—linking electricity with heating, transport, hydrogen, and industrial systems. For instance, PyPSA-Eur-Sec Brown et al. [26] models high-resolution cross-sectoral energy systems for Europe using hourly dispatch and investment optimization Brown et al. [27], Gøtske et al. [28], Unnewehr et al. [29], Glaum et al. [30].
- (iv) Scenario Uncertainty and Flexibility: Increasingly, scenario analysis includes probabilistic methods and stochastic programming to account for uncertainty in inputs. Approaches such as *robust optimization* Conejo and Wu

[31], Qiu et al. [32] and *adaptive scenario trees* Lorca and Sun [33], Moret et al. [34], Li and Grossmann [35], Kayacık et al. [36] are gaining traction to deal with deep uncertainties in renewable integration and technology uptake. (v) Tool Comparison and Benchmarking: Comparative studies, such as those by the European Climate Foundation (ECF) and the Openmod initiative Hilpert et al. [37], have highlighted methodological differences across tools and their implications for policy outcomes Prina et al. [38], Pfenninger et al. [39].

While these models offer quantitative rigor and technical transparency, their interpretability and accessibility for broader stakeholders—such as policymakers, investors, or the public—remain limited. In Göpfert et al. [40] authors introduced datasets designed to help researchers interpret quantitative data. However, these datasets are tailored for expert users and are not easily comprehensible for laypersons. This has prompted a growing body of work focused on enhancing the communicability of model results through *visualization*, *interactive dashboards*, and more recently, natural language generation techniques powered by Large Language Models (LLMs). Table Appendix .1 shows the summary of notable energy-system optimization frameworks.

Despite their analytical rigor and proven utility for long-term planning, traditional energy system optimization models can become prohibitively expensive when applied to fine-grained spatial resolutions, hourly temporal resolutions, or large scenario ensembles Pfenninger et al. [41], Ramsebner et al. [42]. These computational limitations restrict their scalability and responsiveness—especially in interactive policy settings or exploratory modeling under deep uncertainty. To overcome these bottlenecks, recent research has increasingly adopted *machine learning-based surrogate models* as emulators of complex energy system behavior. These surrogates—trained on a subset of high-fidelity model outputs—enable rapid evaluation of scenario outcomes while preserving key system dynamics Yao et al. [43], Grillone et al. [44]. As a result, surrogate modeling plays a vital role in enabling real-time scenario analysis, sensitivity exploration, and the democratization of energy system insights.

Recent literature spans a wide spectrum of machine-learning techniques:

- (i) Tree-based methods: Random-Forest (RF) surrogates have proved robust for grid-related tasks such as low-voltage power-flow emulation Balduin et al. [45] and for thermal-energy-storage CFD emulation where RFs complement neural networks in hybrid workflows Menear et al. [46].
- (ii) Deep Neural Networks (DNNs): Fully connected, convolutional and recur-

rent architectures underpin building-energy calibration Herlinger et al. [47], active-learning optimisation of building envelopes Bamdad et al. [48], and multi-generation energy-system design with six conflicting objectives Ghafarasl et al. [49]. At the systems level, country-scale **EnergyPLAN** runs can be emulated up to two orders of magnitude faster with DNN surrogates Prina et al. [50].

(iii) Hybrid and review studies: Ensemble or hybrid physics–ML schemes accelerate national energy-economic models Bogensperger et al. [51]. Comprehensive reviews now synthesise progress for optimal-power-flow surrogates Mohammadi et al. [52].

(iv) High-dimensional physics: Deep convolutional surrogates have been used for rapid topology-driven heat-transfer design Keramati and Hamdullahpur [53], while climate modellers employ DNNs to emulate precipitation fields in Earth-system models Weber et al. [54].

Collectively, these studies show that surrogate emulation—whether via RFs, gradient-boosted trees, feed-forward DNNs, CNNs, LSTMs, or hybrid architectures—can cut run-times by 90–99 % while maintaining prediction errors below 5–10 % for most energy-system metrics, enabling broader uncertainty analysis, policy exploration, and user-interactive scenario tools.

While surrogate modeling addresses the computational challenges of large-scale simulations, another growing barrier in energy system modeling lies in the interpretability and accessibility of results for diverse stakeholders. Even the most efficient surrogate models often produce outputs that are highly technical and difficult for non-experts—such as policymakers, planners, or the public—to interpret or act upon. To bridge this communication gap, researchers are increasingly exploring the use of LLMs to facilitate model transparency Wasserkrug et al. [55], automate insight extraction, and support interactive, user-centric engagement with complex datasets and optimization outputs. Recent developments demonstrate how LLMs can serve as powerful mediators between technical models and human decision-makers, ushering in a new paradigm of interpretable, conversational modeling interfaces. The rise of LLMs has begun to reshape scientific workflows by automating literature insight, metadata parsing, and stakeholder-focused model communication. Recent initiatives demonstrate this paradigm shift through a suite of domain-tailored LLM applications, several of which are summarized as follows.

(i) Energy Language Model (ELM): Developed by NREL, ELM integrates LLMs (e.g., GPT-4) with energy data sources to enable chat-based querying of large technical corpora. It uses retrieval-augmented generation (RAG) to support

tasks such as legal ordinance extraction and research report summarization with human-level accuracy, improving reproducibility and transparency in energy studies Buster [56], Weers et al. [57].

(ii) *AskGDR assistant*: Extending ELM principles, *AskGDR* is a domain-specific virtual assistant for the Geothermal Data Repository (GDR). By combining metadata and documents with LLM capabilities, it answers semantic researcher queries—on dataset origin, methodology, and applicability—enhancing data discoverability and utility Weers et al. [57].

(iii) *Policy and siting automation*: Demonstrating LLM-based extraction of renewable energy siting ordinances from zoning documents, achieving 85%–90% accuracy vs. manual curation—significantly reducing researcher effort and improving maintainability of policy databases Buster [56], Buster et al. [58].

(iv) *General frameworks*: Broader efforts, like NREL’s Language Model Inventory, survey capabilities and offerings of both open- and closed-source LLMs, presenting strategic insights into their utility for model communication and domain-specific adoption Emami et al. [59].

These studies establish LLMs as powerful tools for automated model communication in science—bridging the gap between technical findings and stakeholders through intelligent document parsing, Q & A interfaces, and policy-focused knowledge extraction. Their emergence suggests promising avenues for enhancing interpretability, accessibility, and democratization of scientific outputs.

1.2. Contributions and Paper Roadmap

However, despite their analytical rigor, traditional energy system models often generate outputs in forms that are difficult for non-expert stakeholders, such as policymakers, urban planners, and community organizations, to interpret or utilize effectively in decision-making contexts Pfenninger et al. [41], Fouquier et al. [60]. As energy transitions become more complex—driven by high shares of variable renewable energy, decentralized infrastructures, and multi-sectoral coupling—there is a growing demand for modeling frameworks that not only provide accurate projections but also offer intuitive, interactive, and explainable outputs Bevis et al. [61], Fontes et al. [62].

In response to this challenge, we introduce *RE-LLM*, a novel hybrid framework designed to enhance the accessibility and interpretability of energy system modeling through the integration of LLMs within classical scenario analysis workflows. *RE-LLM* builds upon recent advances in natural language pro-

cessing and machine learning to couple traditional optimization tools (e.g., GAMS-based models) with post-processing modules for surrogate modeling and automated explanation generation. Specifically, the framework integrates: (i) scenario-based optimization over techno-economic variables and policy constraints, (ii) machine learning surrogates to reduce computational burden and enable real-time sensitivity analysis, and (iii) LLM-powered natural language generation to translate complex model outputs into accessible explanations tailored to diverse user groups.

This integration of LLMs into the modeling pipeline marks a significant step toward human-centric energy planning, where complex quantitative results are rendered transparent and actionable through conversational AI interfaces. By facilitating interactive, multi-lingual, and context-aware exploration of energy futures, RE-LLM contributes to bridging the gap between technical modeling communities and broader stakeholder audiences—thus advancing the co-design of sustainable energy strategies in line with global climate objectives Bouckaert et al. [63], L’Heureux et al. [64].

This paper makes three main contributions:

1. Framework design: We introduce RE-LLM, a hybrid modeling workflow that integrates optimization-based scenario analysis, machine learning surrogates, and LLM-powered explanation in a unified, user-facing pipeline. This design explicitly targets both computational efficiency and interpretability, bridging quantitative rigor with stakeholder accessibility.
2. Demonstration of scalability: We apply RE-LLM in a large-scale energy planning context, showing that machine learning surrogates can accelerate scenario exploration by more than an order of magnitude while maintaining high fidelity to detailed optimization results. This illustrates the framework’s capacity to support rapid, interactive exploration of uncertain futures.
3. Stakeholder validation: Through a structured user study with energy policy analysts, we demonstrate that LLM-generated narratives significantly improve comprehension of complex scenarios compared with traditional numerical or chart-based reporting. This highlights the potential of natural language explanations to democratize insights from energy system modeling.

The remainder of the paper is structured as follows. Section 2 provides an overview of energy system modeling and its role in long-term planning. Sec-

tion 4 introduces the RE-LLM framework, detailing the integration of scenario-based optimization, surrogate modeling, and LLM-driven interpretation. Section 5 presents the simulation results for the case study, demonstrating the framework’s ability to enhance both computational efficiency and stakeholder interpretability. Finally, Section 6 concludes with a summary of contributions and outlines directions for future research.

By merging speed, rigor, and interpretability, RE-LLM aspires to make sophisticated energy modelling as accessible as a conversation—bridging the final mile between data-driven insight and real-world action.

2. Energy System Model Overview

Energy System Optimization Models (ESOMs) are typically formulated as constrained optimization problems, where the goal is to minimize a cost function $f(\mathbf{x})$ subject to a set of feasibility constraints $g_j(\mathbf{x}) \geq 0$ for all $j \in J$. Here, $\mathbf{x} \in \mathbb{R}^n$ is the vector of decision variables representing technology investments, land-use allocations, or energy system flows.

$$\min_{\mathbf{x}} \quad f(\mathbf{x}), \tag{1}$$

$$\text{s.t.} \quad g_j(\mathbf{x}) \geq 0, \quad \forall j \in J, \tag{2}$$

while this general formulation can represent nonlinear optimization problems, most ESOMs adopt an LP structure to ensure tractability and scalability. In the linear case, the objective and constraints are linear functions of the decision vector \mathbf{x} . Specifically:

$$\min_{\mathbf{x}} \quad c^\top \mathbf{x}, \tag{3}$$

$$\text{s.t.} \quad A\mathbf{x} \geq \mathbf{b}, \tag{4}$$

here, $c \in \mathbb{R}^n$ is the cost coefficient vector, $A \in \mathbb{R}^{m \times n}$ is the constraint matrix, and $\mathbf{b} \in \mathbb{R}^m$ encodes lower bounds for the constraints. This structure allows ESOMs to scale to national or continental-level planning horizons, spanning hundreds of technologies and regions.

The LP formulation underpins many established frameworks, including TIMES Loulou et al. [8], MESSAGE Huppmann et al. [9], and BENOPTex Millinger et al. [13], and enables fast solution times using state-of-the-art solvers like CPLEX or Gurobi.

2.1. Case Study: Net-zero emissions

BENOPTex (the *BioENergy OPTimisation* model) is a high-resolution, linear-programming tool that determines the cost-optimal and/or greenhouse-gas-optimal allocation of biomass, hydrogen and excess renewable electricity across the power, heat and transport sectors Millinger et al. [13]. Written in MATLAB and GAMS, it follows every pathway from feedstock to end-use service, comparing more than 30 conversion technologies, over 20 biomass types and a full suite of power-to-X options, all the way down to 15-minute time-steps on the electricity side Millinger et al. [13]. This granularity enables rapid Pareto-front, Monte-Carlo sensitivity and policy-scenario analyses that large integrated-assessment or power-system models typically cannot perform in practical run-times. Originally developed for German energy-transition studies, the framework is country-agnostic and has already informed federal policy on biofuels, heating and electrofuels. For additional flexibility, extensions to this base LP structure often include:

- MILP: Incorporates binary or integer constraints for modeling unit commitment, investment thresholds, or technology activation decisions Floudas and Lin [65].
- Multi-period formulations: Includes inter-temporal coupling (e.g., via storage dynamics or investment rollouts), often spanning multi-decade horizons.
- Stochastic or robust formulations: Used to capture uncertainty in demand trajectories, technology costs, or resource availability Conejo and Wu [31], Forootani et al. [66].

This mathematical backbone forms the core of the RE-LLM framework, upon which surrogate modeling and LLM-based explanation layers are built.

This model presents a cost-optimization framework for evaluating land-based greenhouse gas (GHG) mitigation strategies in Germany’s LULUCF (Land Use, Land-Use Change, and Forestry) sector over the 2020–2050 period. It simultaneously considers FM options (e.g., afforestation, set-aside conservation, peatland rewetting) and agriculture and soils interventions (e.g., agroforestry, cover crops, soil carbon enhancement), each characterized by region- and time-specific cost and abatement profiles. The objective function minimizes total system cost, including both investment and operational

expenditures as well as CO₂ allowance purchases, subject to a series of constraints. These include annual GHG reduction targets, land availability limits, technology adoption rates, and national peatland restoration mandates. By integrating physical, economic, and policy dimensions, the model identifies least-cost deployment pathways while preserving feasibility and equity across space and time. It is intended to support climate policy design, investment planning, and scenario evaluation in alignment with national and European Union (EU) mitigation goals.

2.1.1. Sets

$$\mathcal{T} : \text{Set of years } t = 2020, \dots, 2050 \quad (5)$$

$$\mathcal{R} : \text{Set of regions (e.g., DE1–DEG)} \quad (6)$$

$$\mathcal{F} : \text{Set of Forest Management (FM) options} \quad (7)$$

$$\mathcal{A} : \text{Set of Agriculture and Soils mitigation options} \quad (8)$$

2.2. Parameters

$$\text{costInvLevelFMs}_{t,f,r} : \text{Levelized investment cost of FM [EUR/ha]} \quad (9)$$

$$\text{costMargFMs}_{t,f,r} : \text{Marginal cost of FM [EUR/ha]} \quad (10)$$

$$\text{ghgFMs}_{t,f,r} : \text{GHG removal potential of FM [tCO}_2\text{eq/ha]} \quad (11)$$

$$\text{FMsgrowth}_{t,f,r} : \text{Max growth rate of FM capacity [ha/yr]} \quad (12)$$

$$\text{BeechArea0}_{2020,r} : \text{Available beech land area for set-aside [ha]} \quad (13)$$

$$\text{GrassArea0}_{2020,r} : \text{Available grassland area [ha]} \quad (14)$$

$$\text{Agriarea0}_{2020,r} : \text{Available agricultural area [ha]} \quad (15)$$

$$\text{CO}_2\text{price}_t : \text{CO}_2 \text{ price in year } t \quad (16)$$

$$\text{ghgTargetLULUCF}_t : \text{GHG abatement target in year } t [\text{MtCO}_2\text{eq}] \quad (17)$$

$$\alpha : \text{Fraction of land allowed for rewetting (e.g., } \alpha = 0.05) \quad (18)$$

$$\text{initRewetting} : \text{Initial rewetted area in 2020 [ha]} \quad (19)$$

2.3. Decision Variables

$\text{cap}_f(t, r)$: Implementation area of FM tech f in region r at year t , (20)

$\text{cap}_a(t, r)$: Implementation area of Agri tech a in region r at year t , (21)

$\text{cost}_f(t, f, r)$, $\text{cost}_a(t, a, r)$: Total cost contributions, (22)

$\text{ghgAbate}_f(t, f, r)$, $\text{ghgAbate}_a(t, a, r)$: GHG removed by tech, (23)

$\text{purCO2LULUCF}(t)$: CO₂ allowances purchased to meet the targets [tCO₂eq], (24)

CO₂gapRewt : Additional CO₂ to meet peatland target [tCO₂eq]. (25)

3. Objective Function

The objective function is to minimize total discounted cost over all years:

$$\begin{aligned} \min \text{Total_cost} = \sum_{t \in \mathcal{T}} & \left[\frac{\text{costAnnualFMs}(t) + \text{costAnnualAgri}(t)}{10^6} \right. \\ & \left. + \gamma \cdot \text{CO2price}(t) \cdot \text{purCO2LULUCF}(t) \right], \quad (26) \end{aligned}$$

where the coefficient $\gamma = 1.1$ represents the CO₂ credit price, which is the amount paid to purchase credits from outside the country to meet specified targets. To encourage the use of domestic resources for climate goals, the price of external carbon credits is assumed to be 10% higher than the domestic carbon price in the same year in the base scenarios.

3.1. Constraints on Forest Management GHG Abatement

FM options contribute to GHG abatement through reforestation, set-aside of natural forests, and rewetting of drained peatlands. Each option's potential is quantified by a technology- and region-specific removal factor, which scales with the implemented area. These equations ensure consistency between physical land use and reported emission reductions, enabling accountability in policy assessments.

$$\text{ghgAbate}(t, f, r) = \text{ghgFMs}(t, f, r) \cdot \text{cap}(t, f, r), \quad (27)$$

$$\text{ghgAbateAnnualFMs}(t) = \sum_{f,r} \text{ghgAbate}(t, f, r), \quad (28)$$

$$\text{totGHGabatmentFMs} = \sum_t \text{ghgAbateAnnualFMs}(t). \quad (29)$$

3.2. Agriculture and Soils GHG Abatement

Agriculture and soil-based mitigation options such as agroforestry, cover cropping, and biochar application offer complementary benefits to forest-based strategies. The model quantifies their GHG removal as a product of regional removal factors and adopted land area. This allows a comparative analysis of cost-effectiveness across sectors.

$$\text{ghgAbate}(t, a, r) = \text{ghgAgri}(t, a, r) \cdot \text{cap}(t, a, r), \quad (30)$$

$$\text{ghgAbateAnnualAgri}(t) = \sum_{a,r} \text{ghgAbate}(t, a, r), \quad (31)$$

$$\text{totGHGabatmentAgri} = \sum_t \text{ghgAbateAnnualAgri}(t). \quad (32)$$

3.3. Cost Equations

The total mitigation cost combines levelized capital expenditures (CAPEX) and marginal operational expenditures (OPEX) with a discount rate of 5%. This reflects real-world investment and maintenance requirements for both FM and Agriculture interventions. The separation of cost components ensures flexibility in sensitivity analyses and policy design (e.g., CAPEX subsidies or carbon pricing adjustments).

$$\text{cost}(t, f, r) = (\text{costInvLevelFMs}(t, f, r) + \text{costMargFMs}(t, f, r)) \cdot \text{cap}(t, f, r), \quad (33)$$

$$\text{costAnnualFMs}(t) = \sum_{f,r} \text{cost}(t, f, r), \quad (34)$$

$$\text{cost}(t, a, r) = (\text{costInvLevelAgri}(t, a, r) + \text{costMargAgri}(t, a, r)) \cdot \text{cap}(t, a, r), \quad (35)$$

$$\text{costAnnualAgri}(t) = \sum_{a,r} \text{cost}(t, a, r). \quad (36)$$

3.4. GHG Target Satisfaction (LULUCF Sector)

This constraint ensures that the combined GHG abatement from all land-based options, plus any purchased CO₂ allowances, meets the predefined LULUCF sector targets. It reflects national or EU-level commitments under climate agreements, and allows the model to explore least-cost pathways to compliance.

$$\frac{\text{ghgAbateAnnualFMs}(t)}{10^6} + \frac{\text{ghgAbateAnnualAgri}(t)}{10^6} + \text{purCO2LULUCF}(t) \geq \text{ghgTargetLULUCF}(t). \quad (37)$$

3.5. Peatland Policy Target (2030 National Plan)

The Peatland policy target should satisfy the following constraint:

$$\sum_r \text{ghgAbate}_f(2030, \text{PC_Rewetting}, r) + \text{CO}_2\text{gapRewt} \geq 5 \cdot 10^6. \quad (38)$$

3.6. Land Use Constraints

These constraints safeguard sustainable land use by ensuring that the total area allocated to different mitigation options does not exceed available resources. For example, only a fraction of grassland and agricultural land is made available for reforestation or agroforestry, based on biophysical

feasibility, biodiversity protection, or food security considerations.

$$\sum_{f \in \text{SetAside}} \text{cap}(2050, f, r) \leq \text{BeechArea0}_{2020,r}, \quad (39)$$

$$\sum_{f \in \text{Plantation}} \text{cap}(2050, f, r) \leq 0.1 \cdot \text{GrassArea0}_{2020,r}, \quad (40)$$

$$\text{cap}(2050, \text{PC_Rewetting}, r) \leq \alpha \cdot (\text{Agriarea0}_{2020,r} + \text{GrassArea0}_{2020,r}), \quad (41)$$

$$\text{cap}(2050, \text{Agri01_AGC}, r) \leq 0.1 \cdot \text{Agriarea0}_{2020,r}, \quad (42)$$

$$\text{cap}(2050, \text{Agri05_Agroforestry}, r) \leq 0.1 \cdot \text{GrassArea0}_{2020,r}. \quad (43)$$

3.7. Growth Constraints

Adoption of mitigation measures is constrained by annual growth rates, which represent capacity limitations in terms of labor, machinery, institutional readiness, and ecological factors. These dynamics prevent unrealistic jumps in land use and reflect the inertia of system transformation.

$$\begin{aligned} \text{cap}(t, f, r) - \text{cap}(t-1, f, r) &\leq \text{FMsgrowth}_{t-1,r}, \\ \text{cap}(t, a, r) - \text{cap}(t-1, a, r) &\leq \text{Agrigrowth}_{t-1,r}, \\ \text{cap}(2020, f, r) &= 0, \\ \text{cap}(2020, a, r) &= 0. \end{aligned}$$

4. Scenario-Based Modeling and Interpretation Strategy using RE-LLM Framework

Building on foundational applications of LLMs in scientific and energy domains, we now turn to a domain-specific implementation—RE-LLM—designed to operationalize these capabilities in the context of land-based negative emission optimization. By focusing on the German LULUCF sector, we demonstrate how classical scenario-based optimization, machine learning emulation, and LLM-powered narrative generation can be integrated into a cohesive framework. The following sections detail the individual components of RE-LLM, from GAMS-based scenario optimization to interpretable surrogate modeling and natural language-driven stakeholder interaction.

To systematically analyze the results of scenario-based energy system optimization, we develop a comprehensive computational framework that integrates optimization outputs, structured feature engineering, statistical

correlation analysis, and interpretable machine learning. The key components of this pipeline are: (i) Scenario Generation and Feature Construction, (ii) Correlation and Clustering of Scenarios, (iii) Machine Learning Surrogate Modeling, (iv) Natural Language Querying via LLMs, where will be discussed in details bellow.

4.1. Scenario Generation and Feature Construction

We begin by generating a bank of scenarios using the GAMS-based¹ optimization model, which explores different assumptions on CO₂prices, FM practices, land area availability, and GHG emission targets. For each scenario, key outputs such as abatement levels (ghgAbateFMs) and technology capacities are exported as GDX² files.

From these optimization outputs, we extract relevant parameters and construct structured input-output datasets. Global and regional trends (e.g., trends in CO₂price, BeechArea0, GrassArea0) are computed using moving-window regression techniques. These features are then aligned across scenarios, normalized, and stored in a structured dictionary indexed by scenario name.

While this preprocessing provides a clean and harmonized dataset, the design of features is not merely a technical step but is driven by deeper methodological considerations. In particular, two core scientific motivations guide the feature construction process:

- *Curse of Dimensionality and Redundancy:* Many raw outputs from integrated assessment models exhibit strong temporal autocorrelations and structured inter-regional patterns. Naively using high-resolution time series as learning inputs leads to inflated dimensionality with diminishing information gain, increasing the risk of overfitting, higher sample complexity, and poor generalization across scenarios.
- *Interpretability and Policy Relevance:* From a practical standpoint, interpretable features such as trend slopes, terminal values, or regional

¹General Algebraic Modeling System, is a high-level modeling system used for mathematical programming and optimization problems.

²GAMS Data eXchange, is a binary file format used by the GAMS modeling system to store and exchange data.

aggregates offer more insight to decision-makers than opaque, high-dimensional vectors. This enhances explainability and preserves traceability between the features and underlying policy levers.

This scale of data is problematic for two core reasons: (i) Redundant Information, i.e. many values are temporally or spatially autocorrelated. Including the full time-series as input leads to sparsity in the effective feature space and poor generalization for learning algorithms; (ii) Sample Complexity, i.e. high-dimensional inputs drastically increase the number of samples required to ensure model generalization. This is especially limiting when scenario runs are computationally expensive or limited in scope.

Methodological Approach. We adopted a three-stage strategy to extract and refine features for each scenario:

1. *Temporal Trend Features:* For every region–technology pair and time-series variable (e.g., investment cost, **FM** area), we extracted three summary statistics:
 - Initial value (typically year 2020),
 - Final value (typically year 2050),
 - Slope of the linear trend over the time horizon (via ordinary least squares regression).

These statistics compactly encode long-term trajectories and inter-annual variability (see Figures 3, 1).

2. *Global and Regional Aggregates:* For system-level drivers such as the CO₂ price or LULUCF GHG targets, we computed global trend features and broadcasted them across regions to maintain a uniform feature space (see Figures 7, 8). Additionally, region-level static datasets (e.g., initial agricultural area) were harmonized and merged into each scenario feature array.
3. *Normalization and Scaling:* To ensure numerical stability and mitigate scale-induced biases in downstream models, all numerical features were normalized to the $[0, 1]$ interval using Min-Max scaling, excluding categorical features such as **Region** and **Technology**.

Taken together, these three stages yield a structured and compact feature space that captures both temporal dynamics and structural heterogeneity across scenarios. Rather than simply reducing data dimensionality, the

design ensures that the extracted features remain faithful to the underlying system logic and policy levers. This design balances interpretability and predictive power:

- *Interpretable ML*: Each feature has a direct correspondence to domain concepts (e.g., investment cost growth, land-use potential), supporting explainable AI and policy insight.
- *Scenario Comparability*: Uniform feature extraction across scenarios enables clustering, sensitivity analysis, and meta-modeling across the full scenario space.
- *Model Efficiency*: By distilling temporal data into compact trend summaries, we reduce the dimensionality by more than 95% while preserving signal relevance.

4.1.1. Scenario Generation and Global Sensitivity Design

Starting from a calibrated base scenario, we construct a 26-member experiment

$$\mathcal{S} = \{S01, \dots, S26\},$$

by *multiplicatively* scaling a set of key drivers—carbon price (CO₂ price), forest-management growth ceilings (FMgrowth), available land bases (BeechArea0, GrassArea0), cost coefficients (costInv, costMarg), and the sector-wide mitigation constraint (τ_t^{LULUCF})—with factors $\{0.8, 1.0, 1.2\}$ (and a few stress-test values $\{0.5, 1.3, 1.5\}$)³. The procedure yields a *full-factorial* design in which every input combination is solved on the full 2020–2050 horizon. Although the framework can easily generate hundreds of combinations, restricting the study to *26 well-chosen perturbations* keeps the optimization workload transparent and auditable while still delivering the breadth required for policy analysis. This choice is scientifically defensible for four reasons:

1. *Interaction capture*: simultaneous perturbation of all inputs allows higher-order interactions (e.g. cost \times land, price \times growth) to be learned by the surrogate, avoiding the bias of one-factor-at-a-time sampling.

³A Python routine reads the baseline with `gdxpds`, applies the scaling to the Value column of each symbol, and writes a new GDX whose filename encodes the factors

2. *Uniform hyper-cube coverage*: scaling preserves the empirically calibrated inter-regional ratios while probing the edges of plausible policy and biophysical envelopes, delivering a near-orthogonal skeleton of the input space with only 26 GAMS solves.
3. *Horizon-based robustness*: because each run spans 2020–2050, the bank reveals how early-period shocks propagate into long-term land-use lock-ins or cost escalations, insights that single-year perturbations cannot offer.
4. *Policy traceability*: scenarios are grouped into intuitive themes (unchanged baseline $S11$; single-lever tests $S07 - -S10$; compound high-ambition packages $S24 - -S26$), enabling direct mapping from quantitative outcomes to stakeholder questions and to the narrative layer produced later via the LLM.

Overall, the design is a computationally light proxy for larger Sobol Sobol [67] or Latin-Hypercube McKay et al. [68] experiments, yet retains the statistical power needed for variance decomposition and surrogate training.

4.2. Correlation and Clustering of Scenarios

Let $\mathcal{S} = \{S_1, S_2, \dots, S_N\}$ denote the set of N scenarios. For each scenario $S_i \in \mathcal{S}$, we associate a data matrix $M_i \in \mathbb{R}^{T \times d}$, where T is the number of region–technology–time entries and d is the number of variables of interest. Depending on the analysis, M_i may represent:

- *Input features*: constructed parameters such as CO₂price trajectories, land availability, or marginal abatement costs,
- *Output results*: optimization outcomes such as ghgAbateFMs, cost-TechFMs, or capAgri.

General Method. Each matrix M_i is standardized by applying per-feature z-score normalization⁴, producing \widetilde{M}_i . We then vectorize:

$$m_i := \text{vec}(\widetilde{M}_i) \in \mathbb{R}^{T \cdot d}, \quad \forall i = 1, \dots, N.$$

⁴Z-normalization (standardization) rescales features to zero mean and unit variance Jain et al. [69].

The similarity between any two scenarios S_i and S_j is measured using the Pearson correlation coefficient Pearson [70]:

$$\rho_{ij} := \frac{\langle m_i - \bar{m}_i, m_j - \bar{m}_j \rangle}{\|m_i - \bar{m}_i\| \cdot \|m_j - \bar{m}_j\|},$$

where \bar{m}_i denotes the mean of vector m_i . Collecting all pairwise similarities yields the correlation matrix:

$$C := [\rho_{ij}]_{1 \leq i, j \leq N}.$$

To obtain a dissimilarity measure suitable for clustering, we set:

$$D_{ij} := 1 - \rho_{ij}, \quad \text{for all } i \neq j.$$

Using the condensed form of D , we compute a hierarchical clustering linkage matrix Z with the **average** linkage criterion:

$$Z := \text{linkage}(\text{condense}(D), \text{method} = \text{"average"}).$$

The dendrogram \mathcal{T} derived from Z provides a hierarchical visualization of scenario similarities.

Applications. This general procedure is applied in two complementary ways:

1. *Input-space analysis:* M_i corresponds to the feature matrix X_i , enabling us to cluster scenarios according to their underlying assumptions (e.g., CO₂price trajectories, land use, costs).
2. *Output-space analysis:* M_i corresponds to the output matrix Y_i , allowing us to examine whether distinct input assumptions yield converging or diverging optimal outcomes (e.g., abatement levels, technology capacities).

Together, these analyses reveal both structural similarities in scenario design and functional similarities in optimization results.

4.2.1. Scenario Ranking and Interpretation

Given the correlation matrix $C = [\rho_{ij}]$ derived either from the input features or the optimization outputs (as defined earlier), we aim to identify extremal pairs of scenarios that reflect maximal and minimal similarity. Formally, define the set of all unordered scenario pairs:

$$\mathcal{P} := \{(i, j) \in \{1, \dots, N\}^2 : i < j\}.$$

We then compute the following:

$$\begin{aligned}(\hat{i}_{\max}, \hat{j}_{\max}) &= \arg \max_{(i,j) \in \mathcal{P}} \rho_{ij}, \\(\hat{i}_{\min}, \hat{j}_{\min}) &= \arg \min_{(i,j) \in \mathcal{P}} \rho_{ij}.\end{aligned}$$

Let $\rho_{\max} := \rho_{\hat{i}_{\max}\hat{j}_{\max}}$ and $\rho_{\min} := \rho_{\hat{i}_{\min}\hat{j}_{\min}}$ denote the corresponding correlation values. These pairs indicate, respectively:

- The most similar scenario pair $(s_{\hat{i}_{\max}}, s_{\hat{j}_{\max}})$ under the selected correlation metric, and
- The most dissimilar (potentially outlier) scenario pair $(s_{\hat{i}_{\min}}, s_{\hat{j}_{\min}})$.

Such rankings are instrumental for:

1. identifying clusters of similar behavior in the input or output space;
2. detecting atypical scenarios that diverge from the overall structure;
3. selecting representative scenarios from dense clusters for further interpretability and policy insight.

4.3. Machine Learning Surrogate Modeling.

Let $\mathcal{D} = \{(x_i, y_i)\}_{i=1}^n$ denote a supervised training dataset constructed from scenario-enhanced features and corresponding optimization outputs. Each $x_i \in \mathbb{R}^d$ is a feature vector comprising normalized input attributes (e.g., region, technology, CO₂ price, land use), and $y_i \in \mathbb{R}$ is the target variable, such as capFMs, ghgAbateFMs, or costTechFMs.

We seek to learn a predictive mapping $\hat{y} = f_{\theta}(x)$ that approximates the underlying (black-box) optimization operator $\mathcal{O}(x)$:

$$f_{\theta}(x) \approx \mathcal{O}(x),$$

where θ denotes the parameters of the surrogate model, which can be learned using:

- *Tree-based models*: RF s, Gradient Boosted Trees (e.g., XGBoost),
- *Neural models*: Feedforward Deep Neural Networks (DNNs), LSTMs, Transformers.

To improve generalization and robustness, we employ K -fold ensembling strategies. Specifically, let $\{\mathcal{D}_k\}_{k=1}^K$ denote partitions of the training set \mathcal{D} , and let θ_k be the model parameters trained on the k -th subset. The ensemble prediction is given by:

$$\hat{y}(x) := \frac{1}{K} \sum_{k=1}^K f_{\theta_k}(x),$$

which corresponds to uniform averaging (bagging) over K independently trained models. In the case of tree-based models like RF s, this procedure reflects averaging over randomized decision trees; for neural networks, each f_{θ_k} may correspond to a differently initialized DNN.

Let $\hat{y}_i := \hat{y}(x_i)$ denote the predicted value for test input x_i . We evaluate prediction quality using two standard regression metrics:

$$\begin{aligned} \text{RMSE} &:= \sqrt{\frac{1}{m} \sum_{i=1}^m (y_i - \hat{y}_i)^2}, \\ R^2 &:= 1 - \frac{\sum_{i=1}^m (y_i - \hat{y}_i)^2}{\sum_{i=1}^m (y_i - \bar{y})^2}, \end{aligned}$$

where m is the number of test samples and $\bar{y} := \frac{1}{m} \sum_{i=1}^m y_i$ is the empirical mean of the test targets.

This surrogate modeling strategy enables rapid approximation of optimization outcomes across large scenario banks, reducing computational cost and facilitating downstream tasks such as uncertainty quantification, SHAP-based interpretability, and interactive stakeholder querying via language models.

4.3.1. Interpretability via SHAP Analysis

To interpret the surrogate model’s predictions, we employ SHAP (SHapley Additive exPlanations), a game-theoretic approach for computing feature attributions Lundberg and Lee [71]⁵. Given a predictive model $f : \mathbb{R}^d \rightarrow \mathbb{R}$ and an input $x \in \mathbb{R}^d$, SHAP approximates $f(x)$ using an additive feature attribution model:

$$f(x) \approx \phi_0 + \sum_{j=1}^d \phi_j(x),$$

⁵We adopt the SHAP framework for feature attribution.

where: - $\phi_0 = \mathbb{E}_{x'}[f(x')]$ is the baseline (expected) prediction under the training distribution, - $\phi_j(x)$ is the contribution of feature j to the deviation from the baseline prediction, - and the vector $\phi(x) = (\phi_1(x), \dots, \phi_d(x))$ satisfies local accuracy and consistency properties from cooperative game theory.

In our ensemble framework, where we train a collection of K models $\{f_{\theta_k}\}_{k=1}^K$, we compute SHAP explanations for each model individually and aggregate the results. Let $X^{(\ell)} \subseteq X_{\text{test}}$ be a randomly sampled subset of size m , drawn without replacement. For model k and subset ℓ , let:

$$\Phi^{(k,\ell)} \in \mathbb{R}^{m \times d} \quad \text{with entries} \quad \Phi_{i,j}^{(k,\ell)} = \phi_j^{(k)}(x_i^{(\ell)}),$$

denote the SHAP attribution matrix, where $x_i^{(\ell)} \in X^{(\ell)}$ and $\phi_j^{(k)}$ denotes the SHAP value from model f_{θ_k} .

We compute the average SHAP matrix over L random samples per model:

$$\bar{\Phi}^{(k)} := \frac{1}{L} \sum_{\ell=1}^L \Phi^{(k,\ell)} \in \mathbb{R}^{m \times d}.$$

Then, the final ensemble SHAP explanation is obtained by averaging across the K ensemble models:

$$\bar{\Phi}^{(\text{ensemble})} := \frac{1}{K} \sum_{k=1}^K \bar{\Phi}^{(k)} \in \mathbb{R}^{m \times d}.$$

Each row $\bar{\phi}(x_i) \in \mathbb{R}^d$ of $\bar{\Phi}^{(\text{ensemble})}$ provides a vector of local feature attributions for the prediction $f(x_i)$, enabling granular insight into which features drive the surrogate model's behavior under specific scenario conditions.

This interpretability layer is essential for: diagnosing which features influence optimal decisions (e.g., CO₂ prices, land use constraints), explaining why similar inputs yield different outputs in some scenarios, and supporting transparent communication of results to non-technical stakeholders.

Extension: Global SHAP Values and Theoretical Guarantees. While local SHAP values $\phi_j(x)$ provide per-sample attributions, global feature importance can be assessed by aggregating these values across a population. The global SHAP value of feature j over a test distribution $\mathcal{X}_{\text{test}} = \{x_1, \dots, x_m\}$

is defined as the average absolute contribution:

$$\Phi_j^{\text{global}} := \frac{1}{m} \sum_{i=1}^m |\phi_j(x_i)|, \quad j = 1, \dots, d.$$

Equivalently, for ensemble explanations with matrix $\bar{\Phi}^{(\text{ensemble})} \in \mathbb{R}^{m \times d}$ as defined previously, we compute:

$$\Phi^{\text{global}} := \frac{1}{m} \sum_{i=1}^m |\bar{\phi}(x_i)| \in \mathbb{R}^d,$$

where the absolute value is elementwise. This yields a ranking of features by their average marginal contribution to model predictions across the dataset.

SHAP values arise from the unique solution to the class of additive feature attribution methods that satisfy the following axioms (as shown in Lundberg and Lee [71]):

1. *Local Accuracy (Efficiency)*:

$$f(x) = \phi_0 + \sum_{j=1}^d \phi_j(x), \quad \forall x \in \mathcal{X},$$

ensuring that the model's prediction is decomposed exactly into feature contributions.

2. *Missingness*:

If x_j is missing or not used in f , then $\phi_j(x) = 0$.

3. *Consistency (Monotonicity)*: For any two models f and f' such that:

$$\forall x, \quad f'(x) - f'(x_{-j}) \geq f(x) - f(x_{-j}) \quad \Rightarrow \quad \phi_j^{f'}(x) \geq \phi_j^f(x),$$

the attribution to feature j should not decrease if the marginal contribution of j increases in f' relative to f .

These axioms ensure that SHAP values are the unique solution to the Shapley value problem when applied to machine learning explanations under the additive model assumption:

$$g(x) = \phi_0 + \sum_{j=1}^d \phi_j(x),$$

where $g(x)$ is the interpretable surrogate for $f(x)$.

Consequently, SHAP offers both theoretical rigor and empirical utility for understanding the contribution of features across both local and global levels. The global SHAP vector Φ^{global} directly supports variable importance ranking and sensitivity analysis over scenario-based optimizations.

4.4. Natural Language Querying via LLMs

To bridge quantitative modeling and qualitative stakeholder interaction, we formalize a pipeline for natural language querying using a LLM informed by scenario-based optimization data. Let \mathcal{Q} denote a free-form stakeholder query, such as:

\mathcal{Q} : “What happens if CO₂ price increases by 20%?”

Parameter Extraction. We define a keyword-to-parameter mapping $\mathcal{M} : \mathcal{L} \rightarrow \mathcal{P}$, where \mathcal{L} is a space of linguistic patterns (e.g., “CO2 price”, “investment cost”) and \mathcal{P} is the set of scenario parameters:

$$\mathcal{P} := \{\text{CO}_2\text{price}, \text{FMsgrowth}, \text{costMargAgri}, \dots\}.$$

Given \mathcal{Q} , we apply regular expression matching to identify a corresponding model parameter $p^* \in \mathcal{P}$ and a desired multiplicative change $\lambda > 0$, parsed as:

$$\mathcal{Q} \mapsto (p^*, \lambda), \quad \text{e.g., } \lambda = 1.2 \text{ for } +20\%.$$

Scenario Matching. Let $\mathcal{S} = \{S_1, \dots, S_N\}$ denote the set of all scenarios, each represented by a parameter vector:

$$S_i := (p_1^{(i)}, \dots, p_d^{(i)}) \in \mathbb{R}^d,$$

where $p_j^{(i)}$ is the value of parameter p_j in scenario s_i . Define:

$$\mathcal{S}_{\text{match}} := \left\{ s_i \in \mathcal{S} : \left| \frac{p_i^*}{p^*} - \lambda \right| < \epsilon \right\}$$

as the set of matching or nearest scenarios with respect to p^* , within tolerance $\epsilon > 0$.

Scenario Clustering. Let $C \in \mathbb{R}^{N \times N}$ be the correlation matrix of scenario outputs (or inputs), and $Z \in \mathbb{R}^{(N-1) \times 4}$ the linkage matrix from hierarchical clustering. Using a fixed threshold $t > 0$, we assign each scenario S_i a cluster label:

$$\ell_i := \text{fcluster}(Z, t),$$

with cluster membership $\mathcal{C}_k := \{S_i : \ell_i = k\}$.

The matching scenario set $\mathcal{S}_{\text{match}}$ is then assigned to a dominant cluster \mathcal{C}_{k^*} , from which we extract the cluster-wide scenario descriptions and average correlation:

$$\bar{\rho}_{k^*} := \frac{1}{|\mathcal{C}_{k^*}|^2} \sum_{i,j \in \mathcal{C}_{k^*}} \rho(S_i, S_j).$$

Prompt Construction. We construct a structured prompt $\Pi(\mathcal{Q}, p^*, \lambda, \mathcal{C}_{k^*}, \bar{\rho})$ for the LLM, encoding:

- the original query \mathcal{Q} ,
- matched parameter p^* and requested change λ ,
- representative scenarios from \mathcal{C}_{k^*} ,
- cluster summary statistics (size, average correlation).

LLM Querying. Finally, the prompt Π is submitted to an LLM:

$$\text{LLM}(\Pi) \rightsquigarrow \text{Explanation},$$

which generates a textual response describing expected changes in output quantities (e.g., cost, abatement, land use), derived from trends within the matched cluster. This approach enables a seamless integration of model-driven scenario analytics with human-centered decision support, grounded in optimization results, similarity structure, and interpretable language.

Outlook. This integrated pipeline opens the door to horizon-based optimization and multi-factor sensitivity analysis, allowing researchers and decision-makers to explore a wide range of assumptions and assess their systemic implications in a transparent and data-driven manner. While 26 scenarios are considered in this study for tractability and interpretability, the framework is scalable to a larger scenario bank.

5. Simulation results for the Case Study

As mentioned, in complex systems modeling—such as land-use, forestry, and climate mitigation planning—raw scenario outputs are often high-dimensional, heterogeneous, and temporally rich. A single scenario can yield thousands of data points across multiple indicators, regions, technologies, and time steps. While this level of detail is essential for representing systemic complexity, it presents a fundamental challenge for data-driven analysis: the *curse of dimensionality*.

To address this, we constructed a compact, interpretable, and generalizable set of features via a carefully designed feature engineering pipeline. The objective is not only to reduce the dimensionality of the scenario data but also to capture domain-relevant dynamics (e.g., temporal trends, regional disparities, and cross-technology interactions) that preserve signal fidelity while enhancing learning efficiency.

5.1. Feature Illustration

To illustrate the nature and diversity of the raw scenario inputs before feature engineering, we show a representative subset of time-series and static parameters from the base scenario run of the Zero Negative Emission optimization model in Section 4.1. These variables form the foundational drivers of land-use allocation and mitigation cost outcomes in subsequent analysis.

Figures 1– 2 illustrate *GHG removal, marginal cost, and capacity growth trajectories for FM technologies*. Removal potentials differ both by technology (e.g., rewetting vs. reforestation) and region, with linear growth patterns constrained by annual adoption ceilings. Marginal costs are largely stable for most FM s but escalate significantly for peatland rewetting due to increasing marginal difficulty of restoration. Growth patterns (Figure 1) reflect resource constraints and technology-specific saturation points.

Figures 3 and 5 show the *investment-related cost metrics for FM s*. The *investment level cost* (€/ha) remains relatively stable over time, reflecting technology-specific CAPEX assumptions. In contrast, *total investment costs* (M€/yr) grow as a function of both unit costs and cumulative area expansion.

Figure 6 displays the *initial beech and grassland areas by region* in 2020, which define the upper bounds for set-aside conservation and reforestation measures. Substantial regional disparities are evident, with DE1–DE2 hosting the largest beech areas, while grassland is concentrated in DE2, DE9,

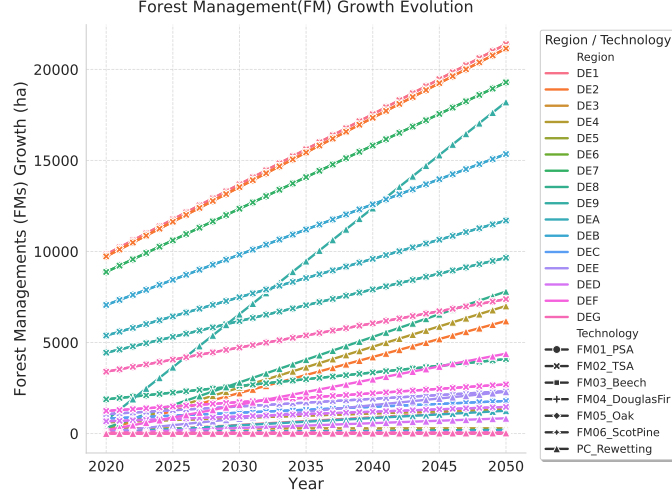


Figure 1: FM capacity growth (ha) by technology and region over 2020–2050. Expansion is constrained by annual adoption ceilings, reflecting practical limits on labor, infrastructure, and ecological readiness.

and DEA. These static land-endowment constraints critically shape feasible deployment paths for FM options.

Figures 8 and 7 present the GHG *target trajectory for the LULUCF sector* and the *CO₂ price path* over 2020–2050, respectively. The targets increase steadily toward 42 MtCO₂eq by 2050, while the CO₂ price rises from below €20/tCO₂ to approximately €250/tCO₂ over the same horizon. Together, these time-series define the policy ambition level and economic incentives for mitigation measures.

These raw variables, along with other scenario parameters (e.g., agricultural mitigation options), are directly extracted from the GAMS model outputs. While each parameter has clear sectoral relevance, taken together they form a high-dimensional dataset. Feature engineering (Section 4.1) condenses these into compact temporal and aggregated descriptors for efficient learning and scenario clustering, without losing interpretability.

Tables 1 and 2 show example feature vectors for Scenario *S10* from the FM scenario bank in Table Appendix .2 and Scenario *S24* from the Agriculture (Agri) scenario bank Table Appendix .2, detailing the complete set of quantitative attributes for a specific region-technology pair under the respective scenario settings. It is worth to highlight that each scenario in FM and Agri has a feature matrix of the size 112×25 and 96×21 , respectively. This

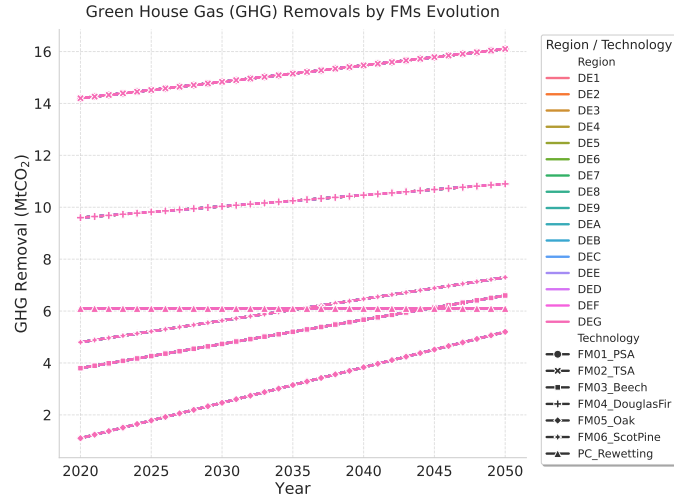


Figure 2: GHG removals by FM technologies and regions over 2020–2050. Growth patterns reflect technology-specific removal factors and capacity adoption limits.

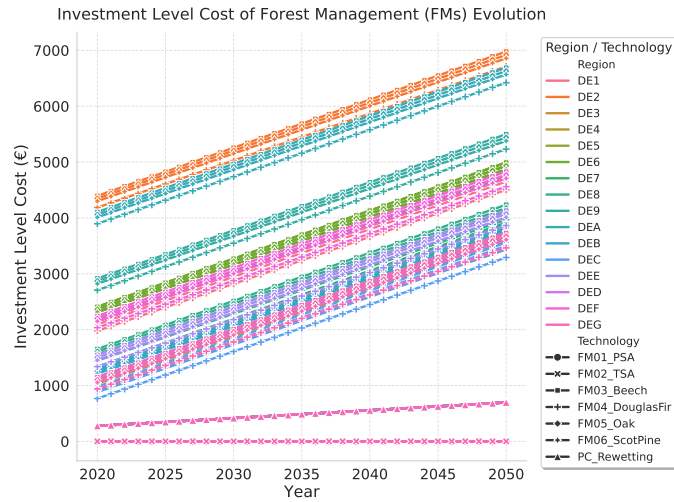


Figure 3: Investment level cost (€/ha) for FM technologies. Assumed constant in real terms for most options, reflecting stable CAPEX assumptions across the planning horizon.

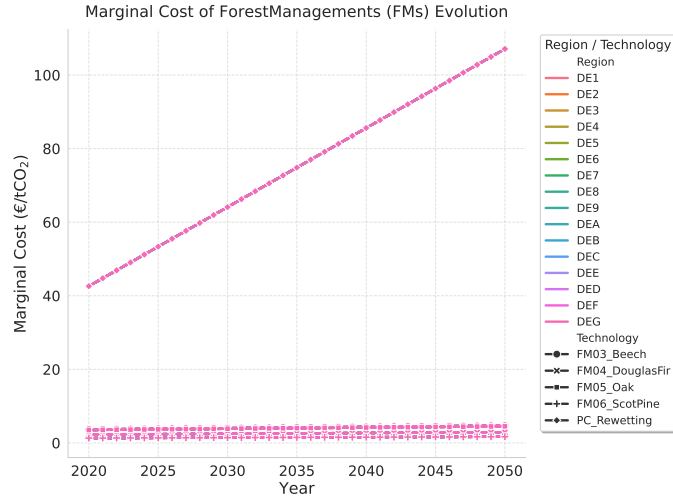


Figure 4: Marginal cost evolution of FM technologies. Peatland rewetting exhibits significant cost escalation over time due to increasing marginal restoration difficulty.

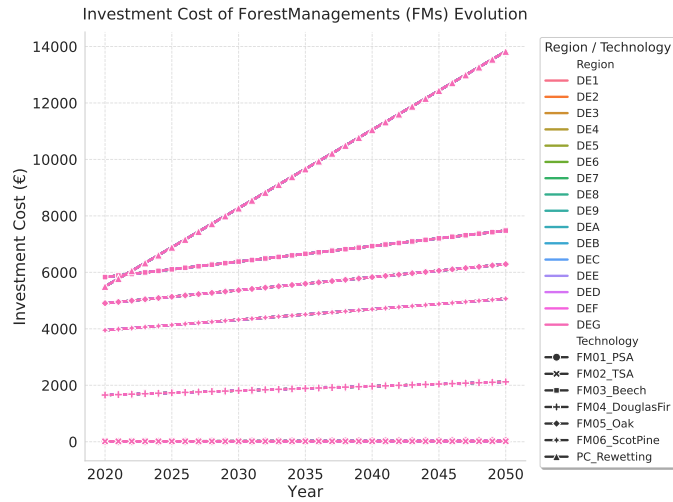


Figure 5: Annual investment costs (M€) for FM technologies. Growth reflects the combined effect of cumulative capacity additions and constant per-unit investment levels.

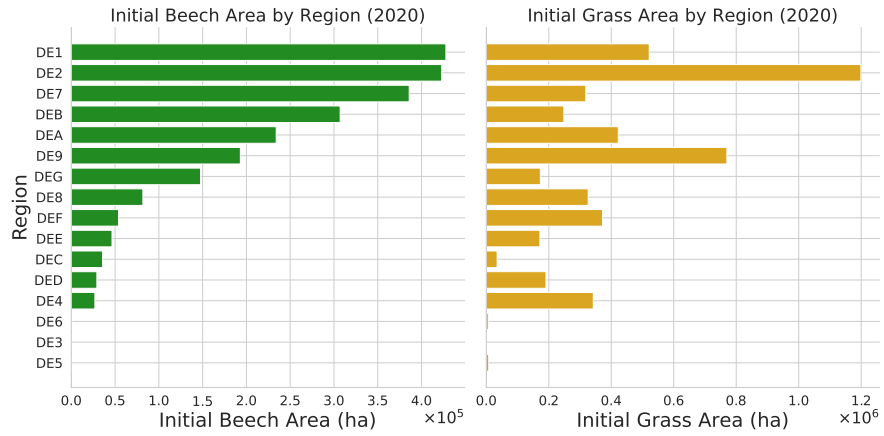


Figure 6: Initial beech and grassland area by region (2020). Static land-use endowments serve as constraints for FM deployment pathways.

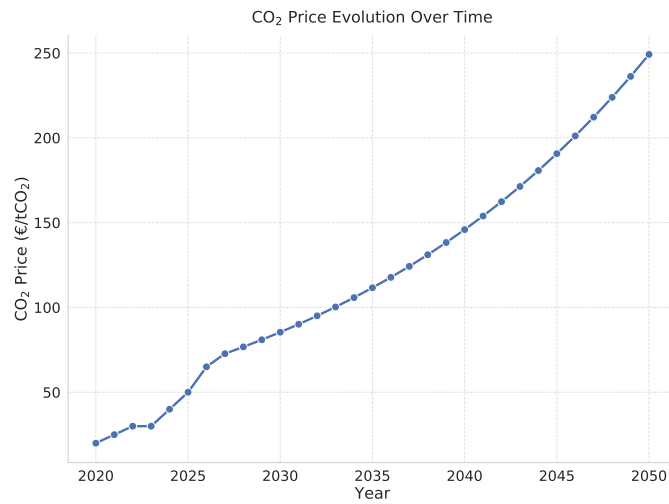


Figure 7: CO₂ price trajectory over 2020–2050. Rising prices strengthen the economic incentive for land-based mitigation measures.

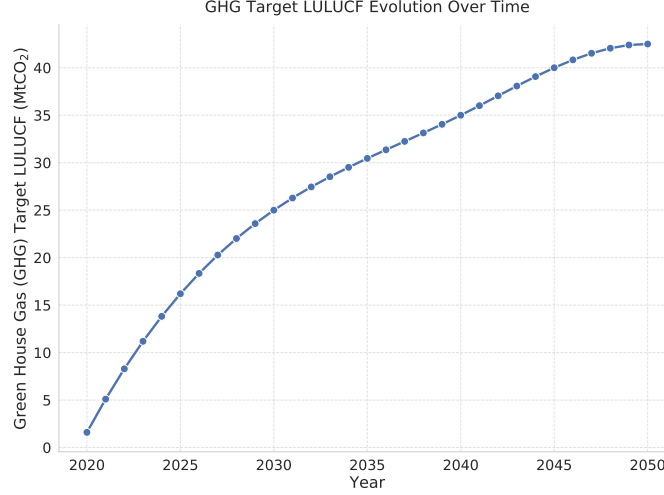


Figure 8: GHG target trajectory for the LULUCF sector over 2020–2050. Increasing targets reflect progressive national and EU climate policy commitments.

shows how feature engineering helps for order reduction in the input dataset.

5.2. Input–Output feature correlation (*Forest Management (FM) vs. Agriculture*)

Both the FM and Agriculture input–feature correlation matrices exhibit *near-perfect* scenario–scenario similarity: almost all off-diagonal Pearson coefficients are $r \approx 0.999$ –1.000, and hierarchical clusters merge at essentially zero height. This pattern implies that scenarios differ mainly by proportional rescalings of the same underlying signals across regions/technologies/years. The combination of multiplicative scenario levers (e.g., uniform scaling of prices, areas, or growth caps) and subsequent feature normalization further compresses variation, inflating collinearity and rendering the scenario space effectively low-dimensional. Practically, both FM and Agriculture inputs form a single dense cluster, so unsupervised grouping provides limited separation and feature-importance attribution may be fragile unless the perturbation design is diversified (e.g., introducing orthogonal shocks by feature group, region-specific shifts, or non-proportional changes).

Input–feature correlation. The correlation matrices for the input features (Figures 9 and 10) reveal extremely high pairwise correlations across the 26 scenarios for both FM and Agriculture inputs. Specifically, the FM input

Table 1: An example of feature vector for Scenario *S10* in the bank of scenarios for FM optimization

Feature	Value
Region	DE2
Technology	FM04_DouglasFir
CostMarg_2020	2.272816
CostMarg_2050	2.914732
CostMarg_Slope	0.021397
CostInv_2020	1654.288462
CostInv_2050	2121.512452
CostInv_Slope	15.574133
CostInvLevel_2020	5023.172313
CostInvLevel_2050	8052.6193
CostInvLevel_Slope	100.981566
GHG_2020	11.52
GHG_2050	13.08
GHG_Slope	0.052
ForestGrowth_2020	10.461851
ForestGrowth_2050	10.461851
ForestGrowth_Slope	0.0
CO2_2020	20.0
CO2_2050	249.197564
CO2_Slope	7.182224
GHGTarget_2020	1.92
GHGTarget_2050	51.0
GHGTarget_Slope	1.495102
InitialBeechArea	423046.85
InitialGrassArea	1199109.02

matrix exhibits correlation coefficients in the range $[0.987, 1.000]$ with an average of 0.999, while the Agriculture input matrix is even more tightly clustered, ranging from 0.9997 to 1.000 with an average of 0.99998. This near-perfect correlation structure reflects the fact that the scenario generation process perturbed key parameters in a highly structured and proportional manner, preserving strong co-movement among input features across scenarios.

Output-feature correlation (costTechAgri and ghgAbateFMs). Unlike the inputs—which form a single, nearly collinear cluster—the *outputs* exhibit clear structure and wider dispersion. The costTechAgri matrix shows several well-separated clusters (dendrogram splits up to noticeable heights), with pairwise correlations ranging from high to only moderate values; small, aligned perturbations in inputs are thus *amplified* by the optimization into distinct cost trajectories. This behaviour is consistent with binding constraints and thresholds (e.g., investment limits, land/area and growth ceilings, carbon-

Table 2: An example of feature vector for Scenario *S24* in the bank of scenarios for Agriculture optimization

Feature	Value
Region	DE3
Technology	Agri01_AG
CostMargAgri_2020	17.25154
CostMargAgri_2050	0.24988
CostMargAgri_Slope	-0.566722
CostInvAgri_2020	2476.190476
CostInvAgri_2050	35.866426
CostInvAgri_Slope	-81.344135
CostInvLevAgri_2020	158.803346
CostInvLevAgri_2050	2.30019
CostInvLevAgri_Slope	-5.216772
GHGAgri_2020	1.8
GHGAgri_2050	1.8
GHGAgri_Slope	0.0
AgriGrowth_2020	20.62545
AgriGrowth_2050	21047.182701
AgriGrowth_Slope	700.885242
Peat_Extraction_2020	0.03
Peat_Extraction_2050	0.3
Peat_Extraction_Slope	0.009
Agriarea0	4836.495

price-driven switching of technologies) that create nonlinear responses: once a constraint activates, marginal costs jump and scenarios diverge.

In contrast, the output correlations (Figures 11 and 12) display greater variability, highlighting the system’s sensitivity to input perturbations. For FM outputs, represented by `ghgAbateFMs`, correlations remain high but show a wider spread ($[0.973, 1.000]$, mean 0.991), indicating that while most FM scenarios respond similarly to input changes, certain combinations of cost, growth constraints, and land availability induce discernible deviations in GHG abatement trajectories. The effect is more pronounced for Agriculture outputs, represented by `costTechAgri`, where correlations span a much broader range ($[0.743, 1.000]$, mean 0.941). This suggests that agricultural technology costs are far more sensitive to input parameter variations, likely due to non-linear cost responses, cross-sectoral interactions, and binding constraints in specific scenarios.

Overall, the comparison between input and output correlation structures underscores two key points: (i) the input space is highly coherent across scenarios by design, ensuring controlled and interpretable perturbations, and (ii) the output space, especially for cost-related agricultural metrics, exhibits amplified differentiation, revealing which parts of the system are most re-

sponsive to policy or techno-economic shifts. This divergence between input uniformity and output variability is precisely what enables the RE-LLM framework to identify and narratively explain the most policy-relevant sensitivities in the LULUCF sector.

5.3. Illustration of ML surrogate Modeling for FM capacity

In order to evaluate the predictive capacity of the proposed feature engineering framework, we construct a supervised learning dataset by combining the scenario outputs from the GAMS-based optimization model with the engineered input features. The raw optimization results are first processed to extract key variables, including CO₂price, FMsgrowth, BeechArea0, and GrassArea0, along with the target variable capFMs. Global and regional trend indicators are subsequently derived using moving-window regressions and integrated with technology–region identifiers to form a structured feature space. All continuous predictors are scaled using min–max normalization, while categorical variables (Region, Technology) are represented through one-hot encoding. The resulting feature arrays are cross-joined with the corresponding years and aligned with observed capFMs values, yielding a consistent input–output dataset for model training.

We employ an ensemble of RF regressors Breiman [72], Pedregosa et al. [73], trained on folded sub-samples of the dataset to ensure robustness against overfitting and to capture non-linear dependencies between features and forest management capacities. Model performance was assessed using out-of-sample predictions, with metrics reported both in normalized units and in original hectares.

In the ensemble training of FM capacity, we employ $n_{\text{folds}} = 10$ (cross-validation) to generate diverse sub-models. Each base learner is a RF Regressor with `n_estimators = 50` trees and varying random seeds across folds to promote model diversity. No explicit constraints on tree depth, minimum split size, or leaf size were introduced. Target values were normalized using Min–Max scaling before training and subsequently inverse-transformed for evaluation. This setup provides a balanced ensemble that emphasizes variance reduction while maintaining computational efficiency.

The ensemble achieved high explanatory power, with R^2 scores exceeding 0.9440 and root mean squared errors (RMSE) on the order of 10150.07 hectares. As illustrated in Figure 13, the predicted values exhibit strong alignment with observed capacities along the 45° reference line. These findings confirm that the engineered scenario features effectively encapsulate the

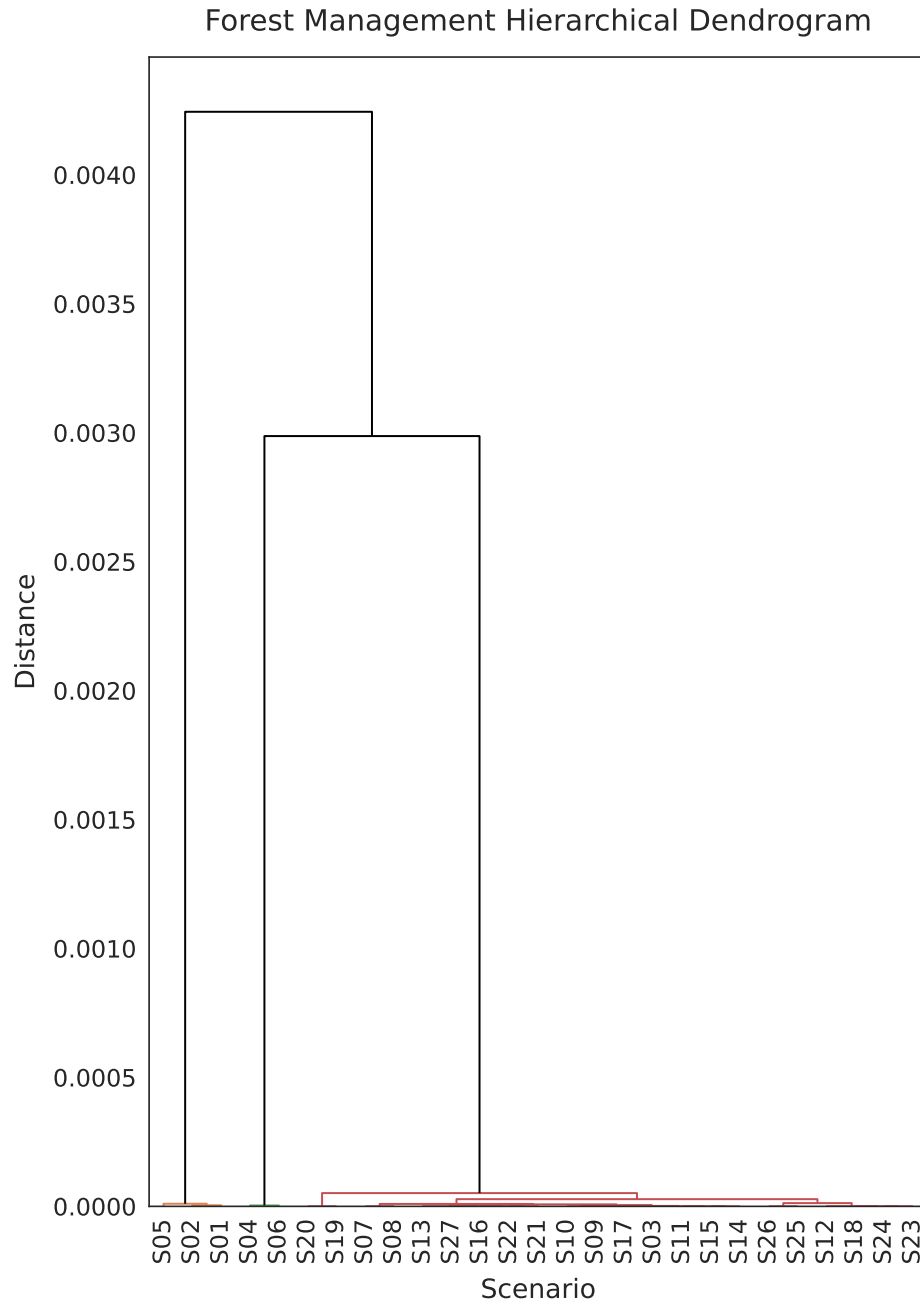


Figure 9: Hierarchical clustering dendrogram from the correlation matrix corresponding to bank of scenarios for the FM .

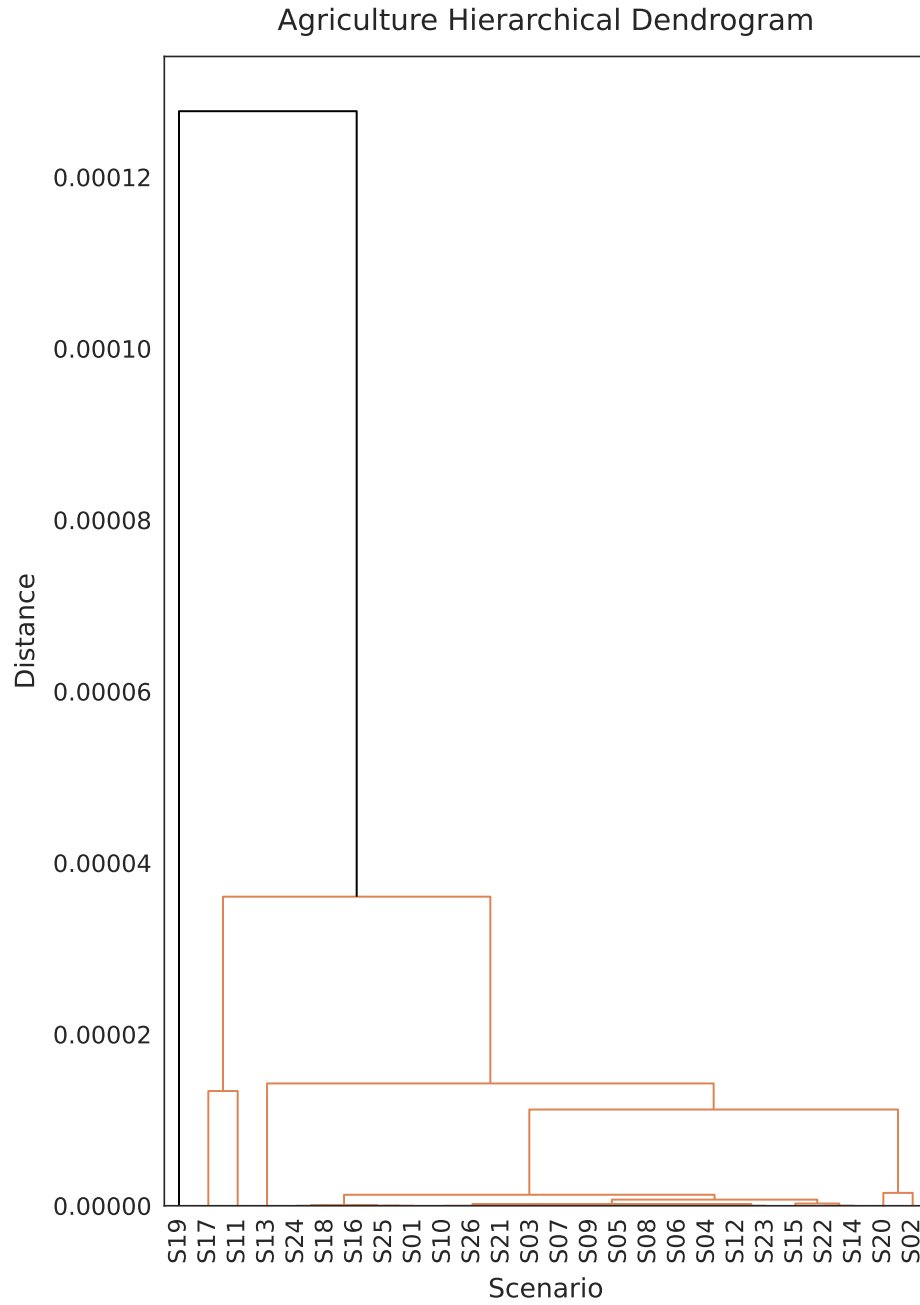


Figure 10: Hierarchical clustering dendrogram from the correlation matrix corresponding to bank of scenarios for the Agriculture optimization.

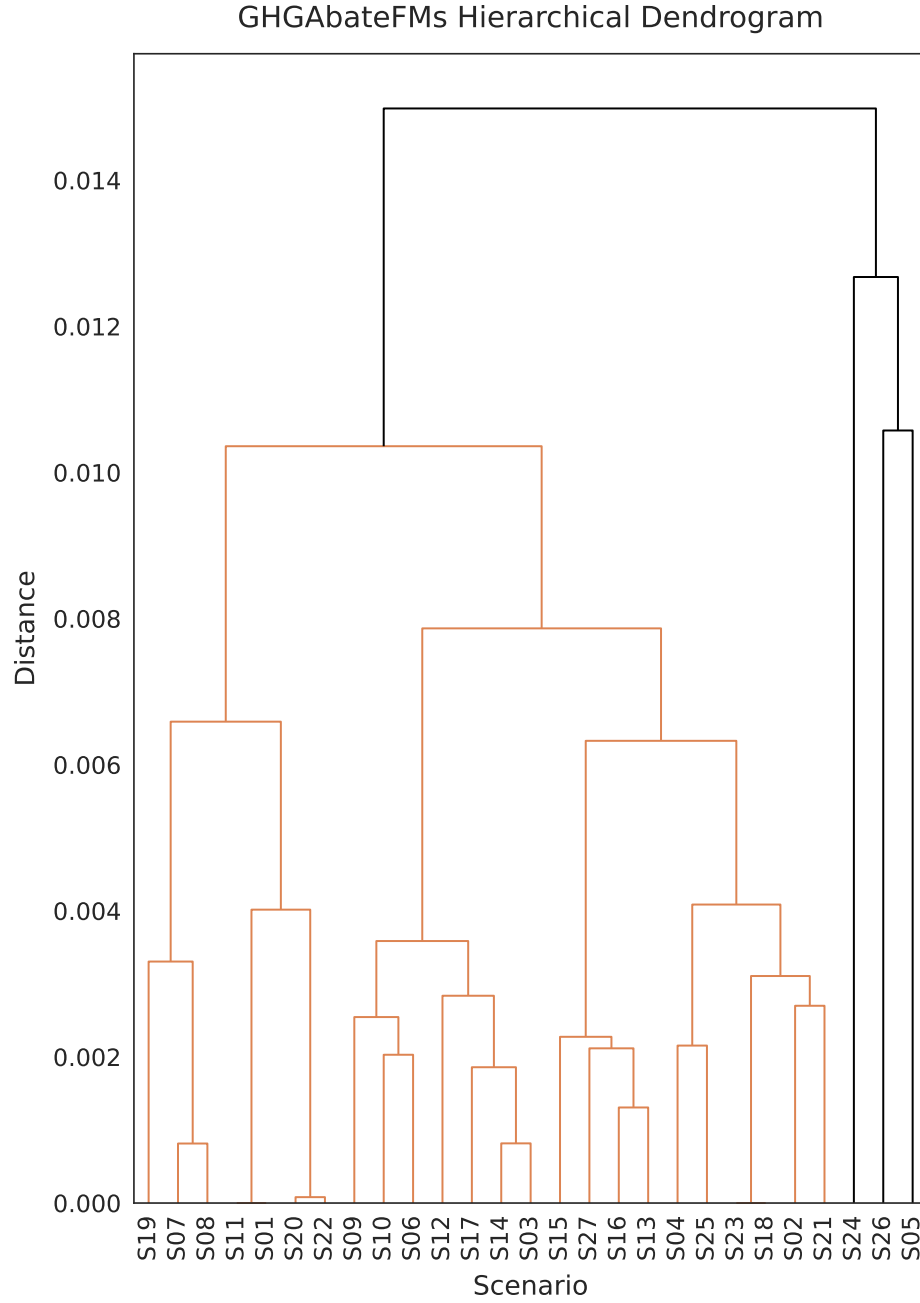


Figure 11: Hierarchical clustering dendrogram from the correlation matrix corresponding to the results of bank of scenarios in the FM for GHGAbateFMs in (27).

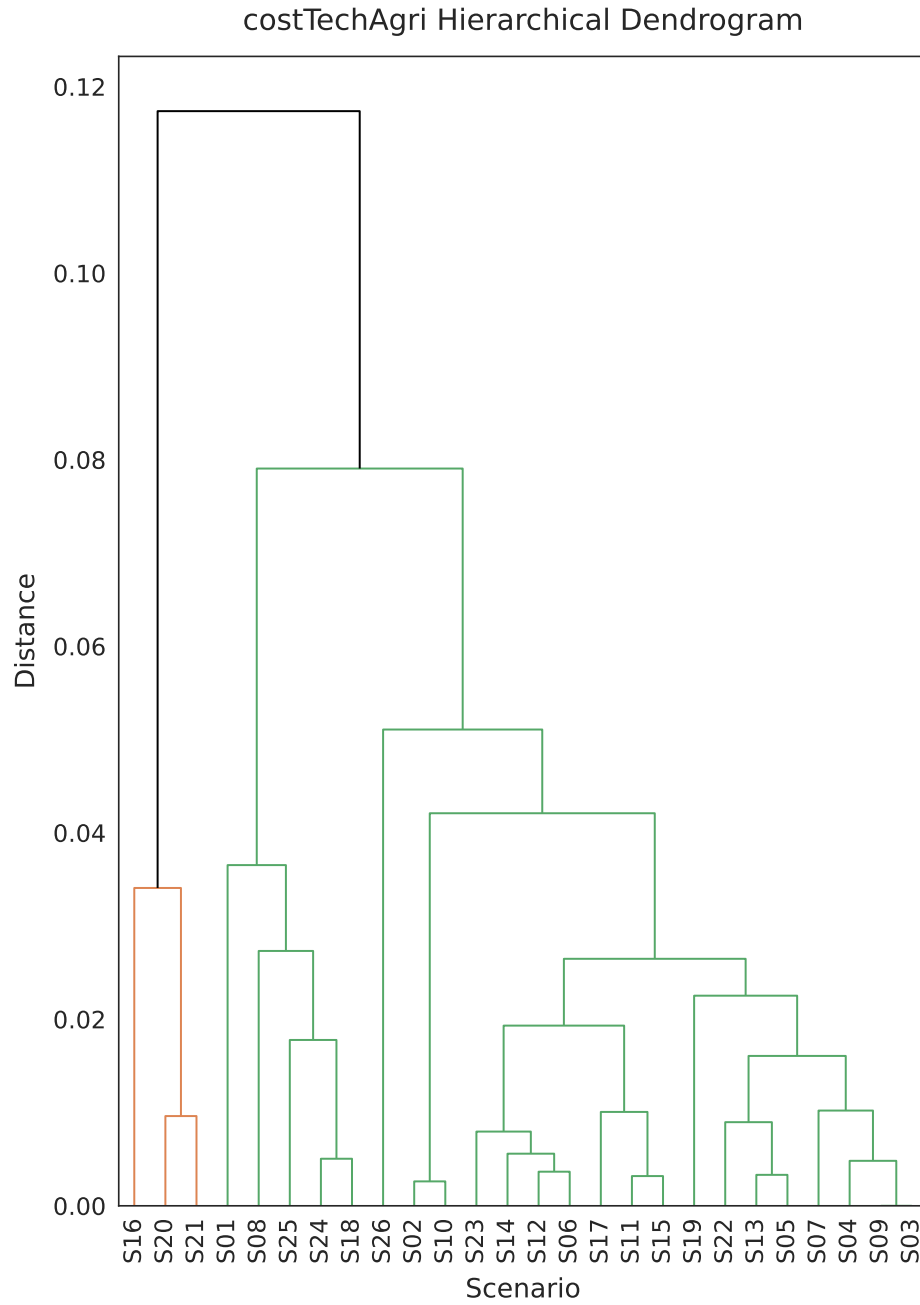


Figure 12: Hierarchical clustering dendrogram from the correlation matrix corresponding to the results of bank of scenarios in the Agriculture optimization for costTechAgri variable.

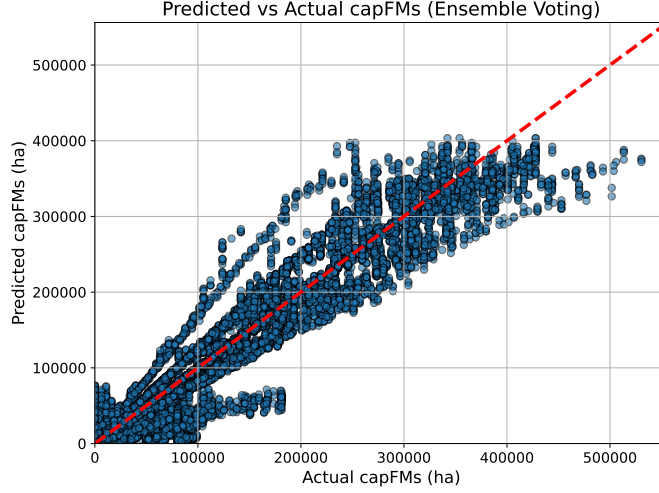


Figure 13: Predicted versus actual values of the FM capacity variable (capFMs) obtained using the RF ensemble model

main drivers of FM capacity, and that the ensemble learning approach yields stable generalization performance across heterogeneous scenario settings.

To interpret the ensemble predictions, we apply SHAP (SHapley Additive exPlanations) using a TreeSHAP approach tailored to the RF regressors. The procedure aggregates explanations across models and repeated subsamples of the test set, ensuring robust feature attribution. Figure 14 illustrates the resulting SHAP summary plot, where each point represents the marginal contribution of a feature to the predicted Forest Management capacity (capFMs). Each point represents the marginal contribution of a feature to the model output across the test data. The horizontal axis indicates the SHAP value (impact on prediction), while the color encodes the feature value from low (blue) to high (red). The most influential drivers are the technology indicator FM02_TSA, temporal effects (year), and investment-related slopes (CostInv_Slope, CostInvLevel_Slope), alongside regional initial conditions such as InitialBeechArea and InitialGrassArea. Positive SHAP values (right side) increase the predicted capacity, while negative values (left side) decrease it, with color encoding reflecting the underlying feature values. This analysis confirms that both cost trends and land endowments interact strongly with regional and technology-specific factors, shaping the optimization outcomes and validating the surrogate model’s interpretability within the RE-LLM pipeline.

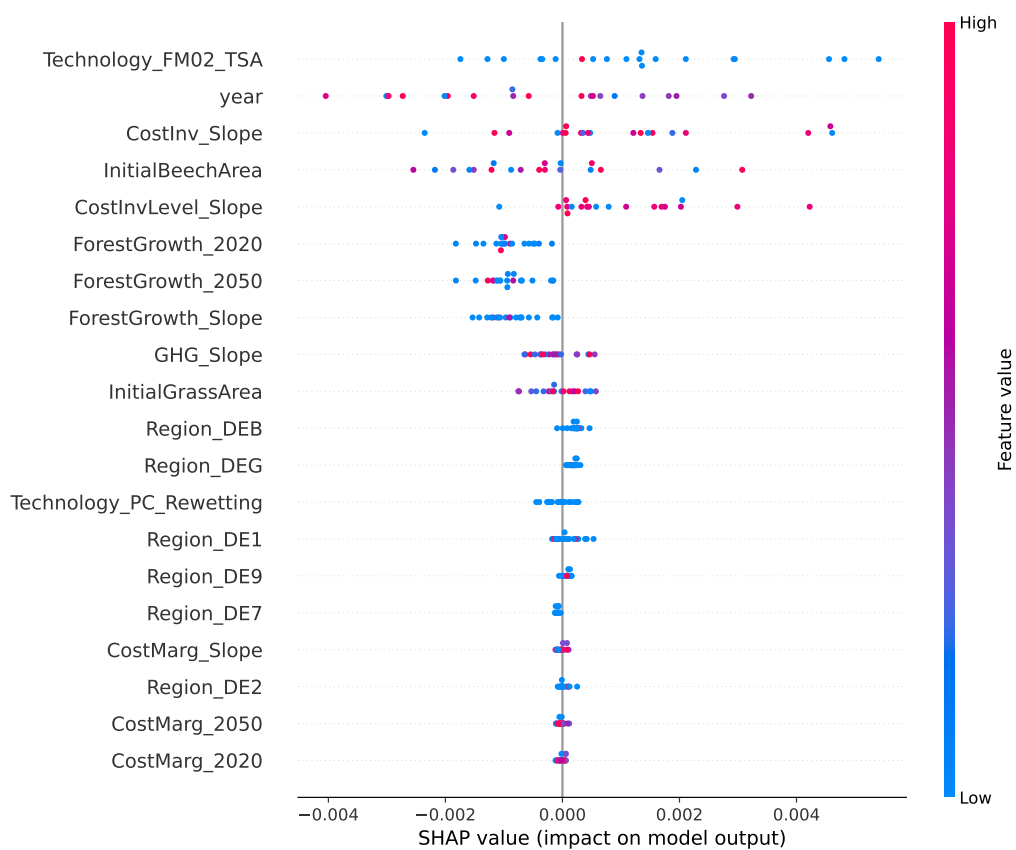


Figure 14: SHAP (SHapley Additive exPlanations) summary plot for the ensemble RF surrogate model predicting FM capacity.

SHAP-guided LLM narratives. To make the language layer faithful to the underlying surrogate, we use SHAP attributions as a structured control signal for prompt construction. Concretely, after computing ensemble SHAP matrices $\bar{\Phi}^{(\text{ensemble})}$ and their global importance Φ^{global} (local accuracy, missingness, and consistency hold by construction), we select the top- k drivers (feature, sign, magnitude, representative value) and serialize them into the LLM prompt used for stakeholder summaries.⁶ In practice, the SHAP summary (e.g., Figure 14 for capFMs) identifies cost trends, land endowments, and technology markers as dominant factors; these are injected into a templated prompt that the LLM converts into a concise, audience-appropriate explanation. By grounding the LLM with SHAP-ranked evidence, the narrative remains traceable to the model’s feature attributions and reduces the risk of free-form speculation—operationalizing the link between interpretable ML and our natural-language interface. In the Appendix Section Appendix .4 a prompt is illustrated to showcase how SHAP analysis can play role in ⁷.

5.4. LLM-driven Stakeholder Interaction

Stakeholders may issue natural language queries, such as “*What happens if CO₂ price increases by 20%?*” or “*What happens if cost of investment in agriculture i.e. costInvAgri decreases?*”. These are mapped to scenario subsets using string parsing and clustering metadata. Prompts are constructed and sent to an LLM, which returns a human-readable summary.

Query 1 — “*What happens if the CO₂ price increases by 20%?*”. The LLM matched this query to scenarios S06–S08, where the carbon-price multiplier is 1.2 while other levers (e.g., FMsgrowth, BeechArea0) vary within their designed ranges. At the cluster level, these runs fall within a coherent group (high intra-cluster correlation), so the narrative reflects behavior that is robust across nearest neighbors. In short, a higher CO₂ price strengthens incentives to deploy land-based mitigation earlier and at larger scale: cumulative GHG abatement rises, reliance on external allowances falls, and technologies with strong abatement per hectare (notably peatland rewetting and set-aside) scale faster subject to land and growth ceilings. Cost trajectories increase

⁶See our SHAP formulation and aggregation across K models and repeated test sub-samples, and the definition of Φ^{global} for population-level ranking

⁷For the LLM query pipeline (parameter parsing, scenario matching/clustering, and prompt construction), see Section 4.4

when adoption fronts meet binding constraints, but the net system-cost pressure is partially offset by reduced purchases of CO₂ credits (the model penalizes external credits relative to the domestic price). The explanation is grounded in the scenario metadata and the correlation-aware clustering used to construct the prompt, ensuring that the textual summary remains traceable to modeled evidence. In Appendix 3 the output of the LLM to this query is shown.

Query 2 — “What happens if the cost of investment in agriculture (`costInvAgri`) decreases?”. For this query, the LLM retrieved the agriculture subset with reduced investment costs (e.g., S10: −50%, S11: −20%, S12: −20% with coupled levers) and composed a response against the same cluster-aware template. Lower `costInvAgri` systematically depresses `costTechAgri` (levelized costs), bringing forward adoption of agricultural mitigation options (agroforestry, cover crops, soil-carbon enhancement) until constrained by land-share and annual growth caps. In turn, the model shifts part of the abatement burden from forest management to agriculture where the marginal abatement cost becomes cheaper, while respecting area constraints and peatland policies. Because agricultural outputs in these experiments exhibit wider dispersion than inputs (optimization non-linearities around binding constraints), the LLM highlights conditionals—where/when the steepest `costTechAgri` declines appear, and which regions/technologies benefit first—and links them to the specific cost-lever scenarios surfaced by the matcher. This keeps the narrative faithful to the designed perturbations while remaining stakeholder-friendly. In Appendix 4 the output of the LLM to this query is shown.

Reproducibility note. Both paragraphs are generated with the documented pipeline: (i) parse the natural-language query to extract parameter changes; (ii) match to nearest scenarios in the bank; (iii) ground the prompt using output-space correlation structure and cluster representatives; and (iv) return an explanation that cites the representative scenarios/clusters. This preserves traceability from the LLM text to the underlying scenario set and clustering artifacts.

6. Conclusion

This paper introduced RE-LLM, a hybrid framework that integrates optimization-based scenario analysis, machine learning surrogates, and large language

models (LLMs) into a unified pipeline for renewable energy and land-use planning. By combining classical GAMS-based optimization with structured feature engineering, correlation and clustering analysis, and surrogate modeling, the framework enables rapid exploration of complex scenario spaces. The LLM layer further enhances interpretability by translating quantitative outputs into accessible narratives tailored to diverse stakeholders.

Through the German LULUCF case study, we demonstrated that surrogate models (RF, DNN, XGBoost) can reproduce optimization outcomes with high fidelity while reducing computational requirements by more than an order of magnitude. SHAP-based interpretability added transparency to model behavior, highlighting the most influential drivers of mitigation costs and capacities. Finally, the LLM-assisted querying pipeline illustrated how natural language interfaces can bridge the gap between technical outputs and actionable insights, thereby improving stakeholder comprehension and engagement.

Overall, RE-LLM advances a human-centric paradigm for energy system modeling, where computational efficiency and interpretability are treated as complementary design goals. By merging speed, rigor, and accessibility, the framework supports interactive, multilingual, and policy-relevant engagement with future energy pathways. Future research will extend this approach toward larger scenario banks, multi-country applications, and deeper integration of LLMs with optimization solvers, ultimately contributing to more transparent and participatory energy transition planning.

Acknowledgment

This study is funded by the *Man0EUvRE* (100695543), which is co-financed by means of taxation based on the budget adopted by the representatives of the Landtag of Saxony. “Man0EUvRE – Energy System Modelling for Transition to a net-Zero 2050 for EU via REPowerEU,” is funded by CETPartnership, the European Partnership under Joint Call 2022 for research proposals, co-funded by the European Commission (GAN°101069750).

Appendix .1. Summary of notable energy-system optimization frameworks

Table .3: Summary of notable energy-system optimization frameworks.

Framework	Licence / language	Coupled sectors	Typical use case	Notable feature(s)
TIMES	Proprietary model generator (GAMS)	Power, fuels, industry, transport, land	National LT planning, marginal CO ₂ pricing	Mature IEA-ETSAP community and large global database Loulou et al. [22], ets [74], wik [75]
MESSAGE-ix Huppmann et al. [9], mes [76, 77]	Open source (Python/GAMS)	Full energy, engineering, economy, environment (E4)	IAM-consistent energy scenarios, SDG co-analysis	Multiregional, perfect-foresight, flexible solver back-end
OSeMOSYS Howells et al. [2]	MIT-style licence (Python/GNU MathProg)	Power, fuels; heat & transport via extensions	Capacity-expansion in data-poor regions	Minimal core; ideal for teaching and rapid prototyping
PyPSA / PyPSA-Eur-Sec Brown et al. [78]	GPL (Python/ Pyomo)	Electricity, heating, transport, hydrogen	High-res European sector coupling (hourly)	Integration with open GIS data; MILP for unit commitment pyp [79]
GenX Hopkins et al. [80]	Apache-2.0 (Julia / JuMP)	Power; emerging heat and hydrogen modules	Flexible-resource valuation, system adequacy	Semi-continuous unit commitment & storage clustering
ReEDS Ho et al. [81]	NREL proprietary (GAMS)	Power; links to e-mobility & fuels via add-ons	U.S. decarbonisation studies, transmission siting	Probabilistic resource-adequacy and zoning algorithm
EnergyPLAN Lund et al. [82]	Freeware GUI (Delphi)	Electricity, DH, transport fuels	Hour-level operational feasibility, policy mixes	“Smart-energy-system” heuristic with excess balancing
GCAM Calvin et al. [83]	BSD-style (C++)	Economy, energy, land-use, water & climate	Integrated land-energy pathways, AFOLU mitigation	Dynamic-recursive market equilibrium approach
PLEXOS Energy Exemplar LLC [84]	Commercial (C#/SQL)	Primarily electricity + gas/water co-simulation	Market dispatch, generation bidding, nodal prices	Sub-hourly chronological LP/MILPengine
urbs Dorfner [85]	MIT licence (Python/Pyomo)	Multi-commodity (electricity, heat, hydrogen)	Urban & regional capacity expansion	Straightforward hourly LP, Pandas native I/O

Appendix .2. Bank of FM and Agriculture scenarios

Table .4: Bank of Scenarios for FM optimization;*Legend: ** = costInvAgri / costMargAgri / costInvLevelAgri / Agriarea0.

Scenario	CO2price	FMsgrowth	BeechArea0	GrassArea0	τ_t^{LULUCF}	cap0FMs	costMargFMs	costInvFMs	costInvLevelFMs	ghgFMs	*
S01	-20%	-20%	-20%	—	—	—	—	—	—	—	—
S02	-20%	0%	-20%	—	—	—	—	—	—	—	—
S03	-20%	0%	0%	—	—	—	—	—	—	—	—
S04	+20%	0%	+20%	—	—	—	—	—	—	—	—
S05	+20%	+20%	-20%	—	—	—	—	—	—	—	—
S06	+20%	+20%	+20%	—	—	—	—	—	—	—	—
S07	—	-20%	—	—	—	—	—	—	-20%	—	—
S08	—	-20%	—	—	-20%	—	—	—	-20%	-20%	—
S09	—	+20%	—	—	—	—	—	—	+20%	—	—
S10	—	+20%	—	—	+20%	—	—	—	+20%	+20%	—
S11	—	-20%	-20%	-20%	-20%	-20%	—	—	—	—	—
S12	—	+20%	+20%	+20%	+20%	+20%	—	—	—	—	—
S13	—	—	—	—	—	—	—	—	—	—	-20%
S14	—	—	—	—	—	—	—	—	—	—	+20%
S15	—	—	—	—	—	—	—	-20%	-20%	—	—
S16	—	—	—	—	—	—	—	-10%	+10%	—	—
S17	—	—	—	—	—	—	—	+20%	+20%	—	—
S18	—	—	—	—	—	—	-50%	-50%	-50%	—	—
S19	—	—	—	—	—	—	-50%	-50%	-50%	-50%	—
S20	—	—	—	—	—	-20%	-20%	-20%	-20%	—	—
S21	—	—	—	—	—	—	-20%	-20%	-20%	-20%	—
S22	—	—	—	—	—	+20%	+20%	+20%	+20%	—	—
S23	—	—	—	—	—	—	+20%	+20%	+20%	+20%	—
S24	—	—	—	—	—	—	+50%	+50%	+50%	—	—
S25	—	—	—	—	—	—	+50%	+50%	+50%	+50%	—
S26	—	+30%	+30%	+30%	+30%	—	—	—	—	—	—

Table .5: Bank of Scenarios for Agriculture Optimization

Scenario	CO2price	FMsgrowth	BeechArea0	costMargAgri	costInvAgri	costInvLevelAgri	ghgAgri	Agrigrowth	Agriarea0	PeatExtract
S01	—	—	—	—	—	—	—	+90%	+90%	+90%
S02	—	—	—	—	—	—	—	-60 %	-60 %	-60 %
S03	-20 %	-20 %	-20 %	—	—	—	—	—	—	—
S04	-20%	0 %	-20%	—	—	—	—	—	—	—
S05	-20%	0%	0%	—	—	—	—	—	—	—
S06	+20%	0%	+20%	—	—	—	—	—	—	—
S07	+20%	+20%	-20%	—	—	—	—	—	—	—
S08	+20 %	+20%	+20%	—	—	—	—	—	—	—
S09	—	—	—	—	—	—	—	—	—	—
S10	—	—	—	—	-50 %	-50 %	-50 %	-50 %	-50 %	—
S11	—	—	—	—	-20 %	-20 %	—	-20 %	—	—
S12	—	—	—	—	-20 %	-20 %	-20 %	—	—	—
S13	—	—	—	—	+20 %	+20 %	—	+20 %	—	—
S14	—	—	—	—	+20 %	+20 %	+20 %	—	—	—
S15	—	—	—	—	-30 %	-30 %	—	-30 %	—	—
S16	—	—	—	—	+70 %	+70 %	—	+70 %	—	—
S17	—	—	—	-40 %	—	—	—	-40 %	—	—
S18	—	—	—	+50 %	—	—	+50 %	+50 %	+50 %	+50 %
S19	—	—	—	+60 %	—	—	—	+60 %	—	—
S20	—	—	—	+100 %	+100 %	+100 %	—	—	—	—
S21	—	—	—	—	—	—	- 50 %	—	—	- 50 %
S22	—	—	—	—	—	—	-20 %	-20 %	-20 %	-20 %
S23	—	—	—	—	—	—	+20 %	+20 %	+20 %	+ 20 %
S24	—	—	—	—	—	—	+50 %	+50 %	+50 %	+50 %
S25	—	—	—	—	—	—	+80 %	+ 80 %	+ 80 %	+ 80 %
S26	—	—	—	—	—	—	+80 %	—	—	+80 %

Appendix .3. Data and code availability

The full implementation of the RE-LLM framework, including scenario generation, feature construction, correlation and clustering analysis, surrogate modeling, and LLM-assisted interpretation, is openly available at Github: <https://github.com/Ali-Forootani/RELLM> and Zenodo Ali-Forootani. (2025) .Ali-Forootani/RELLM:RELLM(v1.0.0).Zenodo.<https://doi.org/10.5281/zenodo.17311775>.

The repository provides a reproducible pipeline that integrates GAMS outputs, structured feature engineering, surrogate modeling (RF , DNN, XGBoost), SHAP-based interpretability, and natural-language querying. All scripts, documentation, and example workflows are included to enable replication and extension of the results.

All .gdx input files, the GAMS optimization code (.gms), and the associated outputs (.gdx/.csv) used in this study are openly available at Zenodo: [10.5281/zenodo.17077632](https://doi.org/10.5281/zenodo.17077632).

Appendix .4. LLM Prompt Example Grounded in SHAP Values

For transparency and reproducibility, we document the exact prompt template used to generate stakeholder-oriented narratives from SHAP analysis. The template is automatically constructed by inserting the top- k SHAP-ranked features, model performance metrics, and scenario-level highlights. An example for the capFMs task is shown below.

Listing 1: Python prompt for stakeholder report

```
prompt = f"""
You are a sustainability analyst preparing a summary report for
stakeholders, based on a machine learning ensemble model and SHAP
analysis focused on forest management capacity (`capFMs`).

**Objective**: Predict and understand the key drivers of forest
management capacity (`capFMs`)

**Model Performance**:
• R2 Score: {results_ensemble['r2_original']:.4f}
• RMSE: {results_ensemble['rmse_original']:.2f} hectares

**Top 3 Influential Features (from SHAP analysis across ensemble models
)**:
1. **{top_feature_names[0]}** - SHAP = {top_shap_vals[0]:.3f}, Avg
value = {top_feature_vals[0]:.3f}
2. **{top_feature_names[1]}** - SHAP = {top_shap_vals[1]:.3f}, Avg
value = {top_feature_vals[1]:.3f}
3. **{top_feature_names[2]}** - SHAP = {top_shap_vals[2]:.3f}, Avg
value = {top_feature_vals[2]:.3f}

**Regional & Policy Highlights**:
• Region with highest capFMs potential: **{best_region}**
• Leading growth technology: **{best_tech}**

**Task**:
Craft a clear and professional report that:
- Summarizes the ensemble model's performance in non-technical terms
- Interprets how the top 3 features influence capFMs outcomes across
the ensemble models
- Highlights regional and technological opportunities
- Recommends actions that align with long-term decarbonization goals
```

The tone should be insight-driven, stakeholder-friendly, and suitable for regional planners, policymakers, and sustainability investors. Avoid equations or technical jargon—focus on actionable insights.

"""

Appendix .4.1. LLM outputs in response to SHAP analysis

This listing illustrates how SHAP-derived feature attributions were integrated into a structured natural-language prompt, ensuring that generated explanations remain grounded in interpretable model evidence. The following shows the LLM response to the prompt 1.

Listing 2: Report on Forest Management Capacity Ensemble Model Analysis

Introduction:

This report summarizes the findings of an ensemble model analysis focused on forest management capacity (`capFMs`). The goal of the analysis was to predict **and** understand the key drivers of `capFMs` **and** identify opportunities **for long-term** decarbonization.

Model Performance:

The ensemble model achieved a high R^2 score of 0.9439, indicating a strong relationship between the **input** features **and** the outcome of `capFMs`. The RMSE of 10159.99 hectares indicates that the model **is** able to accurately predict the `capFMs` values.

Top 3 Influential Features:

The SHAP analysis identified the top 3 features that influence `capFMs` outcomes:

1. ****year****: The year variable had a positive impact on `capFMs`, which suggests that **as** time progresses, `capFMs` **is** expected to increase. This could be due to advancements **in** technology **and** improvements **in** forest management practices.
2. ****Technology\FM02_TSA****: The Technology\FM02_TSA variable had a positive impact on `capFMs`, indicating that the use of this technology could lead to improvements **in** forest management capacity.

3. ****CostInvLevel_Slope****: The CostInvLevel_Slope variable had a negative impact on `capFMs`, suggesting that higher investment costs may hinder the development of forest management capacity.

Regional **and** Policy Highlights:

The analysis identified the region **with** the highest potential **for** `capFMs` development **as** DE1. This highlights the importance of investing **in** forest management capacity **in** this region.

The leading growth technology was identified **as** FM02_TSA, which could be a valuable area of focus **for long-term** decarbonization goals.

Recommendations:

Based on the findings of the analysis, we recommend the following actions:

1. Invest **in** the region **with** the highest potential **for** `capFMs` development (DE1) to improve forest management capacity.
2. Focus on implementing the leading growth technology (FM02_TSA) to improve forest management capacity **and** support **long-term** decarbonization goals.
3. Consider reducing investment costs to improve `capFMs` outcomes.

Conclusion:

The ensemble model analysis identified key drivers of forest management capacity **and** regional **and** technological opportunities **for long-term** decarbonization. The recommendations outlined **in** this report align **with** these findings **and** could **help** improve forest management capacity **and** support **long-term** decarbonization goals.

Appendix .5. LLM outputs in response of stack holder's queries in subsection 5.4

Listing 3: Report on Forest Management Capacity Ensemble Model Analysis

Most similar scenarios: ('S06', 'S04') **with** correlation 1.0000
Least similar scenarios: ('S19', 'S17') **with** correlation 0.9997

Most similar scenarios: ('S09', 'S03') **with** correlation 1.0000
Least similar scenarios: ('S02', 'S01') **with** correlation 0.8805
Scenario Summary:
Matched parameter ****C02price**** altered by *****20 %****.
Matched scenario(s): S06, S07, S08.
Cluster #1 -> contains 26 scenarios (average intra-cluster $\rho = 0.970$).

OpenAI Response:

Implications of a 20% Increase in C02 Price

Summary of Change

The stakeholder has requested an analysis of what happens **if** the C02 price increases by 20%. This change corresponds to the parameter **`C02price`** **and is** represented **in** three scenarios: ****S06****, ****S07****, **and **S08****. These scenarios are part of a cluster **with** a high intra-cluster correlation (0.970), indicating that the outcomes across these scenarios are highly similar.

1. ****Overview of Affected Parameters in the Cluster****

The scenarios **in** this cluster (Cluster ID: 1) are defined **with** the following key parameters:

- ****C02price****: Increased by 20% (**from** base value of 1.0 to 1.2)
- ****FMsgrowth****: Varies between 1.0 **and** 1.2
- ****BeechArea0****: Varies between 0.8 **and** 1.2

This variation **in** FMsgrowth **and** BeechArea0 reflects potential changes **in** forest management **and** land use practices, which can amplify **or** moderate the impact of the increased C02 price.

2. ****Key Impacts of the C02 Price Increase****

a. ****Emissions (GHG)****

- ****General Trend****: A higher C02 price generally encourages a shift

- toward lower emissions, **as** it increases the cost of emitting CO₂.
- **Cluster Implication**: In **all** three main scenarios (S06, S07, S08), the CO₂ price **is** raised to 1.2, likely leading to a **reduction in** greenhouse gas emissions, particularly **from** agriculture **and** land use sectors.
 - **Scenarios S06–S08** show slightly different values **for** **FMsgrowth** **and** **BeechArea0**, so emissions changes will vary slightly, but **all** follow the same general trend of **lower emissions** due to the higher carbon cost.

b. **Land Use**

- **Forest Expansion or Conservation**: The parameter **BeechArea0** indicates a potential expansion of beech forest areas. An increase **in** CO₂ price may incentivize more forested land, which increases carbon sequestration.
- **Agricultural Land Use**: **FMsgrowth** reflects potential changes **in** forest management **and** land use intensity. Higher CO₂ prices are likely to **reduce** intensive agricultural land use **in** favor of **more sustainable and** carbon-friendly land use.

c. **Costs**

- **Increased Cost of Emissions**: The higher CO₂ price directly increases the cost of emissions **in** sectors such **as** agriculture **and** forestry.
- **Mitigation Investments**: Scenarios may reflect increased investments **in** carbon sequestration, afforestation, **or** reduced emissions practices, which **in** turn **increase short-term costs** but may **reduce long-term** environmental **or** regulatory risks.

d. **Agricultural and Forestry Management**

- **Shift in Agricultural Practices**: A higher CO₂ price may lead to a **reduction in** GHG-intensive agricultural practices, such **as** peat extraction **or** intensive livestock production.
- **Forest Management**: The parameter **FMsgrowth** (forest management growth rate) impacts forest carbon storage; higher values (**as in** S07 **and** S08) may imply better forest management, leading to **higher carbon sequestration**.

3. ****Most Closely Aligned Scenarios****

The following scenarios are most closely aligned **with S06, S07, and S08** due to their shared parameters:

- ****S03** and **S04**** (C02price_0.8) – Lower CO2 price, so less impact, but similar structure
- ****S05**** (C02price_0.8, FMsgrowth_1.0, BeechArea0_1.0) – Similar structure but lower CO2 price
- ****S06**** (C02price_1.2, FMsgrowth_1.0, BeechArea0_1.2) – Base case **for** this analysis
- ****S07**** (C02price_1.2, FMsgrowth_1.2, BeechArea0_0.8) – Higher forest growth but lower beech area
- ****S08**** (C02price_1.2, FMsgrowth_1.2, BeechArea0_1.2) – Highest forest growth **and** beech area

4. ****Key Trends Across Cluster****

- ****Reduction in emissions****: Due to higher costs of emissions.
- ****Shift towards sustainable land use****: Expansion of forests (especially beech), **and** reduced GHG-intensive agriculture.
- ****Increased cost of carbon-intensive activities****: Especially **in** agriculture **and** land use.
- ****Enhanced forest management practices****: Especially **in S07 and S08**, where FMsgrowth **is** higher.

5. ****Recommendations for Stakeholders****

- ****Policy Makers****: Consider a CO2 price increase **as** a ****cost-effective tool**** to **reduce** emissions **and** promote sustainable land use.
- ****Agricultural Sector****: Be prepared **for **higher costs**** associated **with** emissions, potentially necessitating a shift towards low-

- emission practices **or** carbon offsetting.
- ****Forestry Sector****: Opportunities **for** ****increased carbon sequestration**** **and** forest management investments due to higher CO2 pricing.

Conclusion

A 20% increase **in** CO2 price leads to ****reduced emissions****, ****shifts in land use toward forested and sustainable practices****, **and** ****higher costs for carbon-intensive activities****. The most closely aligned scenarios (S06-S08) show strong consistency **in** outcomes, **with** ****S08**** being the most ambitious **in** terms of both forest growth **and** land use change. This cluster supports the conclusion that a moderate increase **in** CO2 price can effectively drive sustainability improvements across land use **and** emissions sectors.

Listing 4: Report on Forest Management Capacity Ensemble Model Analysis

Scenario Summary:

Matched parameter ****costInvAgri**** altered by ****20 %****.

Matched scenario(s): S11, S12.

Cluster #1 -> contains 26 scenarios (average intra-cluster $\rho = 0.970$).

OpenAI Response:

****Implications of a 20% Decrease in `costInvAgri`****

This scenario explores the consequences of a ****20% reduction in the cost of investment in agriculture (`costInvAgri`)****. This change **is modeled in **Scenarios S11 and S12****, which are part of a tightly clustered **set** of scenarios (Cluster ID 1, intra-cluster correlation = 0.970), indicating that they are highly similar **in structure and behavior**.

****Key Implications of Lower `costInvAgri`****

1. ****Investment and Agricultural Expansion****

- A lower investment cost **in** agriculture makes it ****more financially attractive**** **for** farmers **and** agricultural investors to expand **or** modernize farming practices.
- This may lead to:
 - Increased agricultural land use (``Agriarea0``)
 - Greater adoption of high-**yield** farming techniques
 - Enhanced use of fertilizers **or** machinery (**as** captured by ``Agrigrowth`` **and** ``ghgAgri``)

2. ****Higher Agricultural Emissions (``ghgAgri``)****

- As agricultural investment becomes cheaper, there **is** likely an increase **in** agricultural activity (e.g., more land **in** cultivation, higher fertilizer use).
- This often leads to a ****rise in** agricultural greenhouse gas emissions (``ghgAgri``)******, especially **in** scenarios like ****S12****, where ``ghgAgri`` **is** also reduced to 0.8 (but still increases **from** baseline due to increased activity).

3. ****Shift in Land Use****

- With agricultural expansion, ****land use changes**** are expected **in** the agricultural sector.
- This may result **in**:
 - Increased pressure on natural ecosystems (e.g., peat extraction, forest conversion)
 - Changes **in** ****BeechArea****, ****PeatExtract****, **and** other land-use indicators (**as** seen **in** similar scenarios)

4. ****Economic and Cost Implications****

- Reduced ``costInvAgri`` implies that ****agricultural investment becomes more affordable****, which may:
 - Drive lower overall costs **in** agricultural systems
 - Influence the ****cost of production**** **and** profitability
 - Potentially **reduce** the ****costMargAgri**** (marginal cost of agriculture) **if** the shift **is** substantial

****Trends Across the Cluster (Cluster ID 1)****

The cluster includes scenarios **with** ****similar sensitivities to `costInvAgri`**, **and** trends across the scenarios show:

- ****Positive feedback**** between reduced `costInvAgri` **and** increased `Agrigrowth`, `Agriarea0`, **and** `ghgAgri`.
- Scenarios **with** ****lower `costInvAgri`** tend to ****increase land-use intensity**** **and** ****greenhouse gas emissions**** from agriculture.
- Many scenarios **in** the cluster also adjust `costInvLevelAgri`, which likely reinforces these trends.

****Shared Scenario Patterns****

Scenario	`costInvAgri`	`Agrigrowth`	`Agriarea0`	`ghgAgri`	Notes
S11	0.8 (-20%)	0.8	0.8	0.8	
	Balanced changes in agriculture and emissions				
S12	0.8	0.8	0.8	0.8	
	Similar to S11				
S13	1.2 (+20%)	1.2	1.2	1.2	
	Opposite direction				
S10	0.5	0.5	0.5	0.5	
	Low cost, low investment				
S14	1.2	1.2	1.2	1.2	
	High cost, high investment				

This indicates a ****strong linear or proportional relationship**** between `costInvAgri` **and** agricultural system intensity.

****Most Closely Aligned Scenarios****

The two main scenarios affected by a decrease **in** `costInvAgri` are:

- ****S11****: `costInvAgri_0.8_costInvLevelAgri_0.8_Agrigrowth_0.8`
- ****S12****: `costInvAgri_0.8_costInvLevelAgri_0.8_ghgAgri_0.8`

These are:

- Identical **in** `costInvAgri` **and** `costInvLevelAgri`
- Slightly different **in** `ghgAgri`, but both reflect the ****same broad**

change **in** agricultural investment cost

Other similar scenarios in cluster:

- **S10** (`costInvAgri_0.5`) - even lower cost
- **S01**, **S02**, **S03**, **S04**, **S05** - also show similar agricultural cost **and** growth patterns
- **S22**, **S23**, **S24**, **S25**, **S26** - show increasing `ghgAgri` **with** increasing `costInvAgri`, suggesting a **positive correlation** between cost **and** emissions

Summary of Key Outcomes

Outcome	Impact
----- -----	
Agricultural Investment	Increased due to lower `costInvAgri`
Land Use	Expansion of `Agriarea0` likely
Emissions	Rise in `ghgAgri` due to higher agricultural activity
Costs	Lower marginal and investment costs in agriculture
Correlation	Strong positive correlation with `Agrigrowth` and `ghgAgri` across scenarios
Aligned Scenarios	S11 and S12 are most directly affected, with S10 and S22-S26 showing related trends

Recommendation for Stakeholders

- If `costInvAgri` decreases, expect **higher agricultural productivity**, **increased land use**, **and** **elevated emissions** unless offset by policy **or** technology changes.
- Monitor how changes **in** `costInvAgri` interact **with** **carbon pricing** **or** **peat extraction** policies, **as** these also influence emissions **and** land use.
- Consider aligning agricultural support policies **with** **sustainability goals** to mitigate unintended environmental consequences of low investment costs.

Let me know **if** you'd like a visual interpretation (e.g., chart of emissions vs. cost changes) or a comparison with the baseline scenario (S09).

References

- [1] A. Forootani, M. Tipaldi, R. Iervolino, S. Dey, Enhanced exploration least-squares methods for optimal stopping problems, *IEEE Control Systems Letters* 6 (2021) 271–276.
- [2] M. Howells, H. Rogner, N. Strachan, C. Heaps, H. Huntington, S. Kypreos, A. Hughes, S. Silveira, J. DeCarolis, M. Bazillian, et al., OSeMOSYS: the open source energy modeling system: an introduction to its ethos, structure and development, *Energy Policy* 39 (2011) 5850–5870.
- [3] S. C. Bhattacharyya, *Energy economics: concepts, issues, markets and governance*, Springer Nature, 2019.
- [4] L. Laveneziana, M. Prussi, D. Chiaramonti, Critical review of energy planning models for the sustainable development at company level, *Energy Strategy Reviews* 49 (2023) 101136.
- [5] A. S. Dagoumas, N. E. Koltsaklis, Review of models for integrating renewable energy in the generation expansion planning, *Applied Energy* 242 (2019) 1573–1587.
- [6] D. Connolly, H. Lund, B. V. Mathiesen, M. Leahy, A review of computer tools for analysing the integration of renewable energy into various energy systems, *Applied energy* 87 (2010) 1059–1082.
- [7] H.-K. Ringkjøb, P. M. Haugan, I. M. Solbrekke, A review of modelling tools for energy and electricity systems with large shares of variable renewables, *Renewable and Sustainable Energy Reviews* 96 (2018) 440–459.
- [8] R. Loulou, U. Remme, A. Kanudia, A. Lehtila, G. Goldstein, *Documentation for the times model part II*, Technical Report, 2005.

- [9] D. Huppmann, O. Fricko, P. N. Kishimoto, V. Krey, K. Riahi, et al., The MESSAGEix integrated assessment model and the ix modeling platform (ixmp): An open framework for integrated and cross-cutting analysis of energy, climate, the environment, and sustainable development, *Environmental Modelling & Software* 112 (2019) 143–156. doi:10.1016/j.envsoft.2018.11.012.
- [10] K. Löffler, K. Hainsch, T. Burandt, P. Oei, C. Kemfert, C. von Hirschhausen, Designing a model for the global energy system—GENeSYS-MOD: An application of the open-source energy modeling system (OSeMOSYS), *Energies* 10 (2017) 1468. doi:10.3390/en10101468.
- [11] M. Barani, K. Löffler, P. C. del Granado, N. Moskalenko, E. Panos, F. M. Hoffart, C. von Hirschhausen, M. Kannavou, H. Auer, K. Hainsch, et al., European Energy Vision 2060: Charting diverse pathways for Europe’s energy transition, *arXiv preprint arXiv:2501.12993* (2025).
- [12] T. Brown, J. Hörsch, D. Schlachtberger, Pypsa: Python for power system analysis, *arXiv preprint arXiv:1707.09913* (2017).
- [13] M. Millinger, P. Tafarte, M. Jordan, F. Musonda, K. Chan, K. Meisel, D. E. Aliabadi, A model for cost-and greenhouse gas optimal material and energy allocation of biomass and hydrogen, *SoftwareX* 20 (2022) 101264.
- [14] S. Pfenninger, B. Pickering, Calliope: a multi-scale energy systems modelling framework, *Journal of Open Source Software* 3 (2018) 825.
- [15] G. Vaidyanathan, Integrated assessment climate policy models have proven useful, with caveats, *Proceedings of the National Academy of Sciences* 118 (2021) e2101899118.
- [16] B. Cointe, The ar6 scenario explorer and the history of ipcc scenarios databases: evolutions and challenges for transparency, pluralism and policy-relevance, *npj Climate Action* 3 (2024) 3.
- [17] D. Huppmann, E. Kriegler, V. Krey, K. Riahi, J. Rogelj, K. Calvin, F. Humpenoeder, A. Popp, S. K. Rose, J. Weyant, et al., Iamc 1.5 c scenario explorer and data hosted by iiasa, (No Title) (2019).

- [18] J. N. Rooney-Varga, F. Kapmeier, J. D. Sterman, A. P. Jones, M. Putko, K. Rath, The climate action simulation, *Simulation & Gaming* 51 (2020) 114–140.
- [19] B. van Ruijven, J. Min, The messageix-globiom model and scenarios for transition risk analysis (2020).
- [20] J. Rogelj, D. Shindell, K. Jiang, S. Fifita, P. Forster, V. Ginzburg, C. Handa, H. Kheshgi, S. Kobayashi, E. Kriegler, et al., Mitigation pathways compatible with 1.5 c in the context of sustainable development, in: *Global warming of 1.5 C*, Intergovernmental Panel on Climate Change, 2018, pp. 93–174.
- [21] D. Klein, G. Luderer, E. Kriegler, J. Streffer, N. Bauer, M. Leimbach, A. Popp, J. P. Dietrich, F. Humpenöder, H. Lotze-Campen, et al., The value of bioenergy in low stabilization scenarios: an assessment using remind-magpie, *Climatic change* 123 (2014) 705–718.
- [22] R. Loulou, U. Remme, A. Kanudia, A. Lehtila, G. Goldstein, Documentation for the times model part ii, *Energy technology systems analysis programme* 384 (2005).
- [23] H. McJeon, J. Edmonds, N. Bauer, L. Clarke, B. Fisher, B. P. Flannery, J. Hilaire, V. Krey, G. Marangoni, R. Mi, et al., Limited impact on decadal-scale climate change from increased use of natural gas, *Nature* 514 (2014) 482–485.
- [24] W. Short, P. Sullivan, T. Mai, M. Mowers, C. Uriarte, N. Blair, D. Heimiller, A. Martinez, Regional energy deployment system (ReEDS), Technical Report, National Renewable Energy Lab.(NREL), Golden, CO (United States), 2011.
- [25] K. Löffler, K. Hainsch, T. Burandt, P.-Y. Oei, C. Kemfert, C. Von Hirschhausen, Designing a model for the global energy system—genesys-mod: an application of the open-source energy modeling system (osemosys), *Energies* 10 (2017) 1468.
- [26] T. Brown, J. Hampp, F. Hofmann, J. Hörsch, M. Maria, F. Neumann, et al., Pypsa-eur-sec: A sector-coupled open optimisation model of the european energy system (2022).

- [27] T. Brown, D. Schlachtberger, A. Kies, S. Schramm, M. Greiner, Synergies of sector coupling and transmission reinforcement in a cost-optimised, highly renewable european energy system, *Energy* 160 (2018) 720–739.
- [28] E. K. Gøtske, G. B. Andresen, F. Neumann, M. Victoria, Designing a sector-coupled european energy system robust to 60 years of historical weather data, *Nature Communications* 15 (2024) 1–12.
- [29] J. F. Unnewehr, M. Schäfer, A. Weidlich, The value of network resolution—a validation study of the european energy system model pypsa-eur, in: 2022 Open Source Modelling and Simulation of Energy Systems (OSMSES), IEEE, 2022, pp. 1–7.
- [30] P. Glaum, F. Neumann, T. Brown, Offshore power and hydrogen networks for europe’s north sea, *Applied Energy* 369 (2024) 123530.
- [31] A. J. Conejo, X. Wu, Robust optimization in power systems: a tutorial overview, *Optimization and Engineering* 23 (2022) 2051–2073.
- [32] T. Qiu, B. Xu, Y. Wang, Y. Dvorkin, D. S. Kirschen, Stochastic multistage coplanning of transmission expansion and energy storage, *IEEE Transactions on Power Systems* 32 (2016) 643–651.
- [33] A. Lorca, X. A. Sun, Multistage robust unit commitment with dynamic uncertainty sets and energy storage, *IEEE Transactions on Power Systems* 32 (2016) 1678–1688.
- [34] S. Moret, F. Babonneau, M. Bierlaire, F. Maréchal, Decision support for strategic energy planning: a complete robust optimization framework, ????
- [35] C. Li, I. E. Grossmann, A review of stochastic programming methods for optimization of process systems under uncertainty, *Frontiers in Chemical Engineering* 2 (2021) 622241.
- [36] S. E. Kayacik, B. Basciftci, A. H. Schrotenboer, E. Ursavas, Partially adaptive multistage stochastic programming, *European Journal of Operational Research* 321 (2025) 192–207.

- [37] S. Hilpert, C. Kaldemeyer, U. Krien, S. Günther, C. Wingenbach, G. Plessmann, The open energy modelling framework (oemof)-a new approach to facilitate open science in energy system modelling, *Energy strategy reviews* 22 (2018) 16–25.
- [38] M. G. Prina, B. Nastasi, D. Groppi, S. Misconel, D. A. Garcia, W. Sparber, Comparison methods of energy system frameworks, models and scenario results, *Renewable and Sustainable Energy Reviews* 167 (2022) 112719.
- [39] S. Pfenninger, L. Hirth, I. Schlecht, E. Schmid, F. Wiese, T. Brown, C. Davis, M. Gidden, H. Heinrichs, C. Heuberger, et al., Opening the black box of energy modelling: Strategies and lessons learned, *Energy Strategy Reviews* 19 (2018) 63–71.
- [40] J. Göpfert, P. Kuckertz, J. M. Weinand, D. Stolten, Wiki-Quantities and Wiki-Measurements: Datasets of quantities and their measurement context from Wikipedia, *Scientific Data* 12 (2025) 1277.
- [41] S. Pfenninger, A. Hawkes, J. Keirstead, Energy systems modeling for twenty-first century energy challenges, *Renewable and sustainable energy reviews* 33 (2014) 74–86.
- [42] J. Ramsebner, R. Haas, A. Ajanovic, M. Wietschel, The sector coupling concept: A critical review, *Wiley interdisciplinary reviews: energy and environment* 10 (2021) e396.
- [43] Z. Yao, Y. Lum, A. Johnston, L. M. Mejia-Mendoza, X. Zhou, Y. Wen, A. Aspuru-Guzik, E. H. Sargent, Z. W. Seh, Machine learning for a sustainable energy future, *Nature Reviews Materials* 8 (2023) 202–215.
- [44] B. Grillone, S. Danov, A. Sumper, J. Cipriano, G. Mor, A review of deterministic and data-driven methods to quantify energy efficiency savings and to predict retrofitting scenarios in buildings, *Renewable and Sustainable Energy Reviews* 131 (2020) 110027.
- [45] S. Balduin, T. Westermann, E. Puiutta, Evaluating different machine learning techniques as surrogate for low voltage grids, *Energy Informatics* 3 (2020) 24.

- [46] K. Menear, D. Duplyakin, M. C. Oliver, M. Shah, M. J. Martin, J. Martinek, K. Nithyanandam, Z. Ma, One System, Many Models: Designing a Surrogate Model for Sulfur Thermal Energy Storage, Technical Report, National Renewable Energy Laboratory (NREL), Golden, CO (United States), 2023.
- [47] F. Herbinger, C. Vandenhof, M. Kummert, Building energy model calibration using a surrogate neural network, *Energy and buildings* 289 (2023) 113057.
- [48] K. Bamdad, M. E. Cholette, J. M. Bell, Building energy optimization using surrogate model and active sampling, *Journal of Building Performance Simulation* 13 (2020) 760–776.
- [49] P. Ghafariasl, A. Mahmoudan, M. Mohammadi, A. Nazarpour, S. Hoseinzadeh, M. Fathali, S. Chang, M. Zeinalnezhad, D. A. Garcia, Neural network-based surrogate modeling and optimization of a multigeneration system, *Applied Energy* 364 (2024) 123130.
- [50] M. G. Prina, M. Dallapiccola, D. Moser, W. Sparber, Machine learning as a surrogate model for energyplan: Speeding up energy system optimization at the country level, *Energy* 307 (2024) 132735.
- [51] A. J. Bogensperger, Y. Fabel, J. Ferstl, Accelerating energy-economic simulation models via machine learning-based emulation and time series aggregation, *Energies* 15 (2022) 1239.
- [52] S. Mohammadi, V.-H. Bui, W. Su, B. Wang, Surrogate modeling for solving opf: A review, *Sustainability* 16 (2024) 9851.
- [53] H. Keramati, F. Hamdullahpur, Deep convolutional surrogates and freedom in thermal design, *Energy and AI* 13 (2023) 100248.
- [54] T. Weber, A. Corotan, B. Hutchinson, B. Kravitz, R. Link, Deep learning for creating surrogate models of precipitation in earth system models, *Atmospheric Chemistry and Physics* 20 (2020) 2303–2317.
- [55] S. Wasserkrug, L. Boussieux, D. Den Hertog, F. Mirzazadeh, Ş. I. Birbil, J. Kurtz, D. Maragno, Enhancing decision making through the

- integration of large language models and operations research optimization, in: Proceedings of the AAAI Conference on Artificial Intelligence, volume 39, 2025, pp. 28643–28650.
- [56] G. Buster, Large language models (llms) for energy systems research, 2023.
 - [57] J. Weers, S. Podgorny, N. Taverna, A. Anderson, S. Porse, G. Buster, Empowering Geothermal Research: The Geothermal Data Repository’s New AI Research Assistant, Technical Report, National Renewable Energy Laboratory (NREL), Golden, CO (United States), 2024.
 - [58] G. Buster, P. Pinchuk, J. Barrons, R. McKeever, A. Levine, A. Lopez, Supporting energy policy research with large language models: A case study in wind energy siting ordinances, *Energy and AI* 18 (2024) 100431.
 - [59] P. Emami, Z. Li, R. Grout, Language Model Inventory v1. 0 [Slides], Technical Report, National Renewable Energy Laboratory (NREL), Golden, CO (United States), 2023.
 - [60] A. Fouquier, S. Robert, F. Suard, L. Stéphan, A. Jay, State of the art in building modelling and energy performances prediction: A review, *Renewable and Sustainable Energy Reviews* 23 (2013) 272–288.
 - [61] Y. Bevis, G. Schaab, V. Rautenbach, S. Coetzee, Expert opinions on using the third dimension to visualise wind speed uncertainty in wind farm planning, *International Journal of Cartography* 3 (2017) 61–75.
 - [62] C. H. d. O. Fontes, F. G. M. Freires, et al., Sustainable and renewable energy supply chain: A system dynamics overview, *Renewable and Sustainable Energy Reviews* 82 (2018) 247–259.
 - [63] S. Bouckaert, A. F. Pales, C. McGlade, U. Remme, B. Wanner, L. Varro, D. D’Ambrosio, T. Spencer, Net zero by 2050: A roadmap for the global energy sector, 2021.
 - [64] A. L’Heureux, K. Grolinger, M. A. Capretz, Transformer-based model for electrical load forecasting, *Energies* 15 (2022) 4993.
 - [65] C. A. Floudas, X. Lin, Mixed integer linear programming in process scheduling: Modeling, algorithms, and applications, *Annals of Operations Research* 139 (2005) 131–162.

- [66] A. Forootani, M. Tipaldi, M. G. Zarch, D. Liuzza, L. Glielmo, A least-squares temporal difference based method for solving resource allocation problems, *IFAC Journal of Systems and Control* 13 (2020) 100106.
- [67] I. M. Sobol, Global sensitivity indices for nonlinear mathematical models and their monte carlo estimates, *Mathematics and computers in simulation* 55 (2001) 271–280.
- [68] M. D. McKay, R. J. Beckman, W. J. Conover, A comparison of three methods for selecting values of input variables in the analysis of output from a computer code, *Technometrics* 42 (2000) 55–61.
- [69] A. K. Jain, R. P. W. Duin, J. Mao, Statistical pattern recognition: A review, *IEEE Transactions on pattern analysis and machine intelligence* 22 (2000) 4–37.
- [70] K. Pearson, Vii. note on regression and inheritance in the case of two parents, *proceedings of the royal society of London* 58 (1895) 240–242.
- [71] S. M. Lundberg, S.-I. Lee, A unified approach to interpreting model predictions, *Advances in neural information processing systems* 30 (2017).
- [72] L. Breiman, Random forests, *Machine learning* 45 (2001) 5–32.
- [73] F. Pedregosa, G. Varoquaux, A. Gramfort, V. Michel, B. Thirion, O. Grisel, M. Blondel, P. Prettenhofer, R. Weiss, V. Dubourg, et al., Scikit-learn: Machine learning in python, the *Journal of machine Learning research* 12 (2011) 2825–2830.
- [74] The integrated markal–efom system (times) model, IEA-ETSAP, 2016. TIMES is a bottom-up, technology-rich model generator using LP over medium-long horizons.
- [75] Times (energy model), Wikipedia, 2025. TIMES succeeded MARKAL in 2008; used in 177 institutions worldwide.
- [76] Messageix documentation, MESSAGE-ix project (IIASA), 2025. Open-source Python/GAMS framework for energy–economy–environment modelling.

- [77] The messageix modelling framework, OpenMODE Initiative / workshop, 2021. All contents are open-source and designed for integrated assessment energy systems.
- [78] T. Brown, J. Hörsch, D. Schlachtberger, PyPSA: Python for power system analysis, arXiv preprint arXiv:1707.09913 (2017).
- [79] Pypsa, Wikipedia, 2025. Python library for power systems, supports electricity, heating, transport, hydrogen; MILP framework.
- [80] Z. R. Hopkins, M. Sun, J. C. DeWitt, D. R. Knappe, Recently detected drinking water contaminants: Genx and other per-and polyfluoroalkyl ether acids, Journal-American Water Works Association 110 (2018) 13–28.
- [81] J. Ho, J. Becker, M. Brown, P. Brown, I. Chernyakhovskiy, S. Cohen, W. Cole, S. Corcoran, K. Eurek, W. Frazier, et al., Regional energy deployment system (reeds) model documentation (version 2020), Technical Report, National Renewable Energy Lab.(NREL), Golden, CO (United States), 2021.
- [82] H. Lund, J. Z. Thellufsen, P. A. Østergaard, P. Sorknæs, I. R. Skov, B. V. Mathiesen, EnergyPLAN–advanced analysis of smart energy systems, Smart Energy 1 (2021) 100007.
- [83] K. Calvin, P. Patel, L. Clarke, G. Asrar, B. Bond-Lamberty, R. Y. Cui, A. Di Vittorio, K. Dorheim, J. Edmonds, C. Hartin, et al., GCAM v5.1: representing the linkages between energy, water, land, climate, and economic systems, Geoscientific Model Development 12 (2019) 677–698.
- [84] Energy Exemplar LLC, Plexos: Energy market simulation software, <https://www.energyexemplar.com/plexos>, 2025. Commercial, supports sub-hourly LP/MIP, zonal & nodal analysis across power, gas, water, and renewables.
- [85] J. Dorfner, urbs: A linear optimisation model for distributed energy systems, <https://github.com/tum-ens/urbs>, 2023. Accessed: 2025-10-10, release v1.0.1, GPL-3.0 license.